Mon. Not. R. Astron. Soc. **000**, 1–?? (2015) Printed 6 January 2016 (MN LATEX style file v2.2)

Large Magellanic Cloud Near-Infrared Synoptic Survey. III. A Statistical Study of Non-Linearity in the Leavitt Laws

Anupam Bhardwaj[1⋆], Shashi M. Kanbur[2], Lucas M. Macri[3], Harinder P. Singh[1], Chow-Choong Ngeow[4] and Emille E. O. Ishida[5]

1. *Department of Physics & Astrophysics, University of Delhi, Delhi 110007, India.*
2. *State University of New York, Oswego, NY 13126, USA.*
3. *Mitchell Institute for Fundamental Physics & Astronomy, Department of Physics & Astronomy, Texas A&M University, College Station, TX 77843, USA*
4. *Graduate Institute of Astronomy, National Central University, Jhongli 32001, Taiwan*
5. *Max-Planck-Institut für Astrophysik, Karl-Schwarzschild-Straße 1, 85748, Garching, Germany*

Accepted 2016 January 5. Received 2015 December 27; in original form 2015 November 2

ABSTRACT

We present a detailed statistical analysis of possible non-linearities in the Period-Luminosity (P-L), Period-Wesenheit (P-W) and Period-Color (P-C) relations for Cepheid variables in the LMC at optical (VI) and near-infrared (JHK_s) wavelengths. We test for the presence of possible non-linearities and determine their statistical significance by applying a variety of robust statistical tests (F-test, Random-Walk, Testimator and the Davies test) to optical data from OGLE III and near-infrared data from LMCNISS. For fundamental-mode Cepheids, we find that the optical P-L, P-W and P-C relations are non-linear at 10 days. The near-infrared P-L and the $W^H_{V,I}$ relations are non-linear around 18 days; this break is attributed to a distinct variation in mean Fourier amplitude parameters near this period for longer wavelengths as compared to optical bands. The near-infrared P-W relations are also non-linear except for the W_{H,K_s} relation. For first-overtone mode Cepheids, a significant change in the slope of P-L, P-W and P-C relations is found around 2.5 days only at optical wavelengths. We determine a global slope of -3.212 ± 0.013 for the $W^H_{V,I}$ relation by combining our LMC data with observations of Cepheids in Supernovae host galaxies (Riess et al. 2011). We find this slope to be consistent with the corresponding LMC relation at short periods, and significantly different to the long-period value. We do not find any significant difference in the slope of the global-fit solution using a linear or non-linear LMC P-L relation as calibrator, but the linear version provides a 2× better constraint on the slope and metallicity coefficient.

Key words: stars: variables: Cepheids, (galaxies:) Magellanic Clouds, cosmology: distance scale.

1 INTRODUCTION

Cepheids are pulsating variables with a well-defined absolute magnitude for a given period and hence exhibit a Period-Luminosity (P-L) relation also known as the Leavitt Law (Leavitt & Pickering 1912). Thus, Cepheids are used as the standard candles and are essential component in determining extra-galactic distances. The non-linearity of the fundamental-mode Cepheid Period-Luminosity relation has been a subject of many studies in the past decade (Tammann, Sandage & Reindl 2003; Sandage, Tammann & Reindl 2004; Kanbur & Ngeow 2005a; Ngeow et al. 2005; Ngeow & Kanbur 2006; Kanbur & Ngeow 2005b; Sandage, Tammann & Reindl 2009; García-Varela, Sabogal & Ramírez-Tannus 2013). Theoretical models were also developed to analyse Period-Luminosity, Period-Color (P-C) and Period-Luminosity-Color (PLC) relations (Bono et al. 1999;

⋆ E-mail: anupam.bhardwajj@gmail.com

Kanbur, Ngeow & Buchler 2004; Kanbur & Ngeow 2006; Kanbur, Ngeow & Feiden 2007). A comparison of the slopes of P-L and P-C relations in the Galaxy and the Large & Small Magellanic Clouds (LMC, SMC) was provided by Tammann, Sandage & Reindl (2003). Similarly, studies of the P-L and P-C relations in the LMC were carried out first by Sandage, Tammann & Reindl (2004) and investigated further with a rigorous statistical approach in a series of papers (Kanbur & Ngeow 2005a; Ngeow et al. 2005; Kanbur & Ngeow 2005b; Ngeow & Kanbur 2006; Kanbur et al. 2007). These authors also extended the analysis to study breaks in P-L, P-C and Amplitude-Color (A-C) relations at various phases of pulsation (Kanbur & Ngeow 2004, 2006; Kanbur et al. 2010; Bhardwaj et al. 2014, and the references therein). A study at BVI_cJHK_s wavelengths was carried out by Ngeow, Kanbur & Nanthakumar (2008), to test the non-linearity in the LMC P-L relations. The counterparts of OGLE-III Cepheids in 2MASS and SAGE catalogs were used to derive P-L relations, and to test for possible non-linearity at 10 days in Ngeow et al. (2009).

In most previous studies (Tammann, Sandage & Reindl 2003; Sandage, Tammann & Reindl 2004, 2009), the test for non-linearities consisted of fitting slopes to data on opposite sides of a break point, deriving their uncertainties, and evaluating their difference in terms of standard deviations. Kanbur et al. (2007) have shown rigorously that this procedure necessarily leads to a greater probability of error than using a statistical test such as the F-test. Thus, this paper concentrates on applying rigorous statistical tests to mean light relations and compares these results to previous work that has studied these non-linearities at different phases. Many researchers have advocated the use of longer wavelengths in P-L distance work since these relations have a lower dependence on metallicity and extinction, a smaller intrinsic dispersion and are supposedly linear (Monson et al. 2012; Ripepi et al. 2012; Inno et al. 2013). For these reasons, we extend our rigorous tests to near-infrared wavelengths.

Kanbur, Ngeow & Buchler (2004); Kanbur & Ngeow (2006); Kanbur, Ngeow & Feiden (2007) studied theoretical nonlinear models of Cepheids with a view of understanding the interaction between the photosphere and hydrogen ionization front and how this may cause possible sharp non-linearities in the P-C relation at various phases. They found that there are distinct phases and period ranges for which this interaction produces a sharp change to the P-C relation. Recently, Bhardwaj et al. (2014) have discussed various non-linearities in the P-C and A-C relations for Cepheids in the Milky Way and Magellanic Clouds at the phases of maximum and minimum light. These results were found to be consistent with the theoretical explanations (Simon, Kanbur & Mihalas 1993; Kanbur, Ngeow & Buchler 2004; Kanbur & Ngeow 2006; Kanbur, Ngeow & Feiden 2007) relating the hydrogen ionization front and the stellar photosphere and the properties of the Saha ionization equation. The P-L and P-C relations at mean light are usually obtained by the numerical average of the corresponding magnitudes and colors at every phase during a pulsation period. Therefore, any changes in P-C and P-L relations at particular phases during the pulsation cycle can indeed have effects on the mean light P-C and P-L relation. P-C relations can affect the P-L relations through PLC relations and hence it is essential to investigate the various non-linearities in P-L and P-C relations at mean light. We also include reddening independent P-W relations in our analysis.

Motivated by the aforementioned reasons, we use light curve data having full phase coverage to extend our work for the first time to investigate observational evidence for non-linearity in near-infrared P-L, P-W and P-C relations. We combine optical data from the OGLE-III survey (Soszynski et al. 2008; Ulaczyk et al. 2013) with data from the Large Magellanic Cloud Near-Infrared Synoptic Survey (LMCNISS, Macri et al. 2015, and erratum, hereafter, Paper I). We use the F-test, random walk, testimator and Davies tests to determine possibly statistically significant breaks in the P-L, P-W and P-C relations for fundamental and first-overtone mode Cepheids. This paper presented as the third in the series, extends the work of Paper I and Bhardwaj et al. (2015a, hereafter, Paper II) and uses the catalog to study non-linearity in the Leavitt Law. The near-infrared P-L and P-W relations derived in Paper I and II based on our data are very important in distance scale applications and, therefore, a rigorous analysis of non-linearity is essential to avoid any discrepancies in Cepheid based distance estimates.

The paper is structured as follows. In Section 2, we present details of the photometric data and extinction corrections. In Section 3, we describe the various statistical methods used to test the presence and significance of non-linearities in the P-L, P-W and P-C relations. In Section 4, we present the results of our analysis. We also discuss the impact of observed non-linearities on the distance scale. We summarize all the results and the conclusions from this study in Section 5.

2 DATA AND EXTINCTION CORRECTION

The photometric mean magnitudes for optical V- and I-band for Cepheids in the LMC are taken from the Optical Gravitational Lensing Experiment (OGLE - III) survey (Soszynski et al. 2008). There are 1849 fundamental (FU) and 1238 first-overtone (FO) mode Cepheids in the LMC. The optical bands sample will be referred to as "OGLE-III" in this work. We augment this sample with mean magnitudes for 26 long period Cepheids in the LMC from the OGLE-III Shallow Survey (Ulaczyk et al. 2013). The photometric system is exactly similar for both datasets and hence the combined sample will be referred to as "OGLE-III-SS".

The mean magnitudes for the LMC in the optical bands are corrected for reddening using the maps of Haschke, Grebel & Duffau (2011). The color excess $E(V\text{-}I)$ values are obtained from these Haschke maps using RA/DEC for Cepheids in the LMC taken from the OGLE-III database[1]. We corrected mean magnitudes using the Cardelli, Clayton & Mathis (1989) extinction law $A_\lambda = R_\lambda E(B\text{-}V)$, where $E(V\text{-}I)$ is related to $E(B\text{-}V)$ by the relation $E(V\text{-}I) = 1.38E(B\text{-}V)$ (Tammann, Sandage & Reindl 2003). For the LMC, the values for total-to-selective absorption (R_λ) are $R_V = 2.40, R_I = 1.41$, corresponding to $E(V\text{-}I)$ color excess values.

[1] `http://dc.zah.uni-heidelberg.de/mcextinct/q/cone/info`

We use our recently released data from the LMC Near-infrared Synoptic Survey to determine the significance of possible non-linearities in these relations for FU and FO mode Cepheids. The observations for these Cepheids along with their calibration into the 2MASS photometric system, adopted reddening law and extinction corrections are discussed in detail in Paper I. The final sample used in calibrating P-L relations includes 775 FU and 474 FO mode Cepheids in the LMC, which was used to derive P-W relations in Paper II.

3 THE STATISTICAL TESTS

3.1 F-test

Our interest for the present study is to test whether the P-L, P-W and P-C relations display statistically significant evidence of a change of slope. We make use of the method adopted by Kanbur & Ngeow (2004) and used in Bhardwaj et al. (2014) to investigate possible breaks in period-color and amplitude-color relations. We plot the reddening-corrected magnitudes and colors against $\log(P)$ to find P-L and P-C relations. The null hypothesis is that in the reduced model, we can fit a single regression line over the entire period range. The alternative hypothesis is that in the full model, we can fit two separate regression lines for stars with periods on opposite sides of an assumed break point P_b. We assume the reduced model to be the best fit under the null hypothesis. We write the reduced model as:

$$Y = a + b\log(P); \quad \text{For all } P. \tag{1}$$

While the full model is written as:

$$\begin{aligned} Y &= a_S + b_S\log(P); \quad \text{where } P < P_b, \\ &= a_L + b_L\log(P); \quad \text{where } P \geqslant P_b. \end{aligned} \tag{2}$$

Here, Y is the dependent variable, i.e. the magnitude when considering P-L relations, Wesenheit magnitudes (Madore 1982) in the case of P-W relations and the color in the case of P-C relations. The value of the F-statistic is calculated using the following equation :

$$F = \left(\frac{RSS_R - RSS_F}{RSS_F}\right)\left(\frac{\nu_F}{\nu_R - \nu_F}\right), \tag{3}$$

Here, RSS denotes the residual sums of squares, ν is the number of degrees of freedom, and subscripts R and F denote the reduced and full models, respectively. We compare the observed value of F with the values obtained from the F-distribution under the null hypothesis at a given significance level. A larger value of F leads to the rejection of the null hypothesis (see, Bhardwaj et al. 2014).

We note that the parametric F-test is sensitive to the number of and nature of Cepheids on either side of the break period (Kanbur & Ngeow 2004). Thus, samples with fewer data points, say at the long period end, or samples with outliers, will have a higher variance which will make it harder for the F-statistic to be significant. The assumptions underlying the F-test are homoskedasticity, independent identically distributed observations and normality of residuals. Bhardwaj et al. (2014) have demonstrated that OGLE-III data do satisfy these assumptions though there are some departures by a few outliers. In order to strengthen our conclusions, we also apply a number of other tests that do no rely on these assumptions.

3.2 Random walk method

A more robust and simple approach is to study partial sums of the residuals of the least-square fits. The F-test can be affected by the distribution of the residuals from the linear fit. However, the non-parametric random walk test generates the distribution of the residuals from the data itself and, hence, provides a more robust test statistic. This test was used by Koen, Kanbur & Ngeow (2007) to test the non-linearity of OGLE and MACHO V-band P-L relations and is outlined in brief here.

As a first step, the data is sorted according to the increasing value of the period such that, $P_1 < \cdots < P_N$, where N is the total number of stars in the sample. If r_k are the residuals obtained from the linear fit to P-L relations in the form of equation 1, then the partial sum of residuals is

$$C(j) = \sum_{k=1}^{j} r_k. \tag{4}$$

If there is no departure from the linearity, then $C(j)$ is a simple random walk. However, if there is a deviation from linearity $C(j)$ will not be a simple random walk. The reason is that the successive residuals may be correlated unlike in the case of a random walk, where the partial sums are uncorrelated random numbers. To quantify this, our test statistic is the vertical range of $C(j)$, i.e.

$$R = max[C(j)] - min[C(j)]. \tag{5}$$

If the partial sums are a random walk, R will be small. Now to determine the significance level for the R-values, we use the permutation method, as the theoretical distribution of the test statistic of $C(j)$ is not known. We permute r_k such that it randomizes the residuals and destroys any possible trends. We estimate the theoretical R value from the partial sums of permuted residuals and repeat this procedure for a large number (~ 10000) of permutations. We find the proportion of permutation R-values that exceed the observed value obtained using equation 5. This fraction provides the significance level $p(R)$, the p-value for the test statistic. $p(R)$ is the probability of the observed statistic under the null hypothesis (linearity); therefore, the smaller the value, the higher the likelihood of non-linearity.

3.3 The testimator

We also use the test estimator or "testimator" (Kanbur et al. 2007) to analyse the non-linearity of P-L, P-W and P-C relations at mean light. A brief overview is given here. Again, all the data are sorted in order of increasing period. The entire sample is then divided into n different non-overlapping, and hence completely independent subsets. Each subset includes N number of data points and the remaining number of data points are included in the last subset. We fit a linear regression in the

form of equation 1 to the first subset and determine a slope $\hat{\beta}$. This initial estimate (testimator) of the slope is taken as β_0 in the next subset, under the null hypothesis that the slope of the second subset is equal to the slope of the first subset, i.e. $\hat{\beta} = \beta_0$. The alternate hypothesis is that the two slopes are not equal. For hypothesis testing, we calculate the t-statistic, such that -

$$t_{obs} = \frac{(\hat{\beta} - \beta_0)}{\sqrt{(MSE/S_{xx})}}, \tag{6}$$

where,

$$MSE = \frac{1}{N-2}\sum_{i=1}^{N}(Y_i - \hat{Y}_i)^2,$$

$$S_{xx} = \sum_{i=1}^{N}(X_i - \bar{X})^2.$$

Here, $\hat{Y}_i$ represents the best fit linear regression and $\bar{X}$ represents the mean value of independent variables. Since there will be $n_g = n - 1$ hypothesis testing in total, $t_c = t_{\alpha/2n_g,\nu}$, and ν is the number of data points in each subset. We adopt a value of $\alpha = 0.05$ to have a confidence level of more than 95%. Once we know the observed and critical value of the t-statistics, we can determine the coefficient $k = \left(\frac{|t_{obs}|}{t_c}\right)$, which is the probability that the initial guess of the testimator is true. If the value of $k < 1$, the null hypothesis is accepted and we derive the new testimator slope for the next subset using the previously determined $\beta's$ such that -

$$\beta_w = k\hat{\beta} - (1-k)\beta_0. \tag{7}$$

This value of the testimator is taken as β_0 for the next subset. This process of hypothesis testing is repeated n_g times or untill the value $k > 1$, suggesting rejection of the null hypothesis. Then we accept the alternate hypothesis that the data is more consistent with a non-linear relation.

3.4 Segmented lines and the Davies test

An alternative approach to the problem of identifying the existence of a break point is presented in Muggeo (2003). The method first performs a linear piecewise regression considering the existence of the break. Thereafter, the Davies test is used to evaluate if the two segments are different enough to account for two separate linear behaviours[2].

The regression is performed through the use of Generalized Linear Models (GLM), a powerful regression tool widely used in statistics but only recently introduced in astronomy (see e.g. Raichoor & Andreon 2012; de Souza et al. 2015, and references therein). In this framework each observation is interpreted as a realization of a random variable and, consequently, can be described through the determination of its underlying probability distribution function (Hardin & Hilbe 2012).

[2] The method is implemented in the `R` package SEGMENTED (Muggeo 2008).

Consider that the relationship between period ($X = \log(P)$, explanatory variable) and magnitudes/colours (Y, response variable) in equation 2 can also be described as:

$$Y = a_S + b_S X + \Psi(X)\Delta a\,(X - X_b)\,, \tag{8}$$

where $\Delta a = a_L - a_S$, and

$$\Psi(X) = 0; \quad \text{if } P < P_b,$$
$$= 1; \quad \text{if } P \geqslant P_b.$$

The above expression assumes, beyond the existence of the break, a continuous transition between the two linear behaviours. If we want to describe a more general situation, where there is a gap in the intersection, the model can be written as

$$Y = a_S + b_S X + \Psi(X)\left[\Delta a\,(X - X_b) - \gamma\right], \tag{9}$$

where γ represents the magnitude of the gap. The SEGMENTED method uses Equation (9) as a linear predictor for a GLM with identity link function (for a simple introduction to the GLM approach written for astronomers, see, Elliott et al. 2015, section 2).

The algorithm begins with an initial test point $\tilde{P}_b$ and uses the data to fit the other parameters in equation (9). A new break point is updated at each iteration, $\hat{P} = \tilde{P} + \gamma/\Delta a$. The process is repeated until $\gamma \approx 0$, or in other words, when the two lines meet in the estimated break point. The uncertainty in the determination of the break is given by $\hat{\gamma}/\Delta a$ (Muggeo 2008).

Once the regression is done, our final goal is to test if the difference between the two line segments is evidence of distinct underlying linear behaviours. In other words, we wish to test the null hypothesis:

$$H_0 : \Delta a(X_b) = 0, \tag{10}$$

where the parameter of interest, Δa, depends on the break point, X_b. This is the ideal case for the application of the Davies test (Davies 1987). It assumes a χ^2 distributed likelihood whose maximum is determined by the algorithm described above ($\hat{\Delta a}$). Given a test statistics ($S(\bullet, X_b)$) and a list of potential break points $X_t = \{X_1, X_2, ..., X_T\}$, Davies test states

$$\text{p-value} \geqslant \mathcal{N}(-M) + \frac{V\exp\left(-M^2/2\right)}{\sqrt{8\pi}}, \tag{11}$$

where $\mathcal{N}(\bullet)$ is the standard Normal distribution, $M = \max(|S(X_b, X_t)|)$ and V is the total variation of the test statistics, $V = \sum_{i=2}^{T}|S(X_b, X_i) - S(X_b, X_{i-1})|$ (Davies 1987).

The choice of test statistic is itself a free parameter, the only requirement being that it must follow a normal distribution for fixed X_b. In the results presented here, we use the Wald statistic, which evaluates a test point by determining how far it is from the maximum likelihood estimates (MLE). Given the effect of large variances in the shape of the likelihood function, the absolute distance between test and MLE must be weighted by the likelihood variance. Thus, the same distance which might lead us to reject the test point

Table 1. Results of the F-test and random walk test to discern a non-linearity at a period of 10 days on the "simulated" P-L relations.

Y	b_{all}	σ_{all}	N_{all}	b_S	σ_S	N_S	b_L	σ_L	N_L	F	$p(F)$	$p(R)$
V_L	-2.709±0.020	0.210	1776	-2.724±0.035	0.209	1611	-2.671±0.085	0.222	165	0.215	0.806	0.786
V_{NL}	-2.759±0.020	0.214	1776	-2.984±0.035	0.209	1611	-2.541±0.085	0.222	165	31.558	0.000	0.000

Notes: b, σ and N refer to the slope, dispersion and number of stars, respectively. The subscripts all, S and L refer to the entire period range, short period range and long period range, respectively. $p(F)$ and $p(R)$ represent the probability of acceptance of null hypothesis i.e. linear relation.

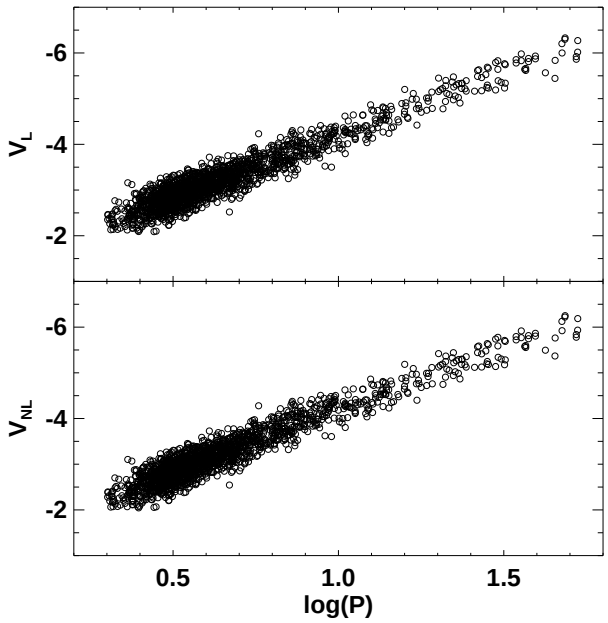

Figure 1. Simulated P-L relations for OGLE-III-SS dataset. We use the equations given in Ngeow & Kanbur (2006) to develop a linear (V_L) and a non-linear (V_{NL}) relation.

for a tightly peaked likelihood can be judged acceptable for a broader one. In this framework, $S(X_b, X_t) = \hat{\Delta}a(X_b)/\sigma$, where $\hat{\Delta}a$ is the MLE value for the difference in slopes and σ is the variance of its likelihood function[3].

4 ANALYSIS AND RESULTS

4.1 Simulated P-L relations

In order to check the accuracy of our statistical tests, we simulate two "artificial" data sets of P-L relations: one linear and one non-linear. The details of the procedure to simulate P-L relations are provided in Ngeow & Kanbur (2006). We use the equations provided in that paper to simulate data, but take the periods from the OGLE-III-SS sample because it spans a wider range and has a greater number of long-period variables. We also add the internal dispersion ($\sigma = 0.20\ mag$) and the photometric error ($0.05\ mag$) to the simulated P-L relations. A plot of our simulated linear and non-linear P-L relations is presented in Fig. 1. The two panels in this figure look very similar but are indeed generated differently and demonstrate why, in the era or precision cosmology, it is vital to determine non-linearities in P-L/P-W/P-C relations rigorously.

We use our statistical tests on these simulated data sets to determine the reliability of our procedures, with the results given in Table 1 for the F-test and random walk, in Table 2 for the testimator and in Table 3 for the Davis test. We find that for a linear relation, the F-test, random walk and the Davis test provide a high p-value, and hence we accept the null hypothesis of a linear P-L relation. Similarly, the testimator accepts the null hypothesis over all period bins. Thus, these test results correctly predict a linear relation. When the true underlying relation is non-linear, the significance probabilities are zero for the F-test, random walk and Davis test, clearly allowing us to reject the null hypothesis and suggesting a non-linearity. Similarly, the testimator rejects the null hypothesis in a period bin that contains the break period of 10 days. Thus our test statistics provide consistent results for the known datasets.

4.2 Optical-infrared P-L, P-W and P-C relations

We apply the tests described in the previous section to various combinations of optical and near-infrared observations to investigate the non-linearity of P-L, P-W and P-C relations at mean light. We derive new P-L and P-C relations at optical wavelengths using both OGLE-III and OGLE-III-SS samples. We apply reddening corrections using maps taken from Haschke, Grebel & Duffau (2011) and a reddening law from Cardelli, Clayton & Mathis (1989). We derive the Wesenheit magnitude $W_{V,I} = V - R(V - I)$ for each sample, where $R = 1.55$ is the color coefficient obtained using the adopted reddening law. We remove 2.5σ outliers to fit P-L, P-W and P-C relations at optical wavelengths.

However, for near-infrared band data, we use the final sample of 775 FU and 474 FO stars as provided in Paper I, since sigma-clipping and extinction corrections were already applied in that work. This final sample was used to derive P-L relations in Paper I and P-W relations in Paper II. We remove 2.5σ outliers to fit a P-C relation at these wavelengths. Similarly, in case of optical-infrared P-W and P-C relations, we apply reddening corrections and 2.5σ clipping before fitting a linear regression to these relations. We also impose an upper limit on periods of 80 days in all these relations to avoid possible contamination from Ultra Long Period Cepheids (ULPCs, Bird, Stanek & Prieto 2009): these stars follow a shallower P-L relation. We do not consider FU

[3] It is important to emphasis that in this context, the algorithm will always return parameters for the two segmented lines. If the Davies test indicates that the break does not exist, fit parameters may be unstable for consecutive runs, even though the final result is not (since in this case there is no break).

Table 2. Results of the testimator on "simulated" P-L relations.

Band	n	$\log(P)$	N	$\hat{\beta}$	β_0	$\lvert t_{obs}\rvert$	t_c	k	Decision	β_w
V_L	1	0.30223−0.43358	175	-3.283±0.377	—	—	—	—	—	—
	2	0.43359−0.47278	175	-1.416±1.208	-3.283	1.546	2.843	0.544	Accept H_0	-2.268
	3	0.47279−0.50185	175	-0.815±1.762	-2.268	0.825	2.843	0.290	Accept H_0	-1.846
	4	0.50186−0.53508	175	-1.541±1.514	-1.846	0.201	2.843	0.071	Accept H_0	-1.825
	5	0.53509−0.57406	175	-3.708±1.258	-1.825	1.497	2.843	0.527	Accept H_0	-2.816
	6	0.57407−0.62397	175	-1.941±0.921	-2.816	0.950	2.843	0.334	Accept H_0	-2.524
	7	0.62398−0.68130	175	-2.840±0.800	-2.524	0.395	2.843	0.139	Accept H_0	-2.568
	8	0.68131−0.77611	175	-2.959±0.533	-2.568	0.735	2.843	0.258	Accept H_0	-2.669
	9	0.77612−0.94936	175	-3.109±0.309	-2.669	1.425	2.843	0.501	Accept H_0	-2.890
	10	0.94937−1.72354	201	-2.758±0.058	-2.890	2.293	2.838	0.808	Accept H_0	-2.783
V_{NL}	1	0.30223−0.43358	175	-3.543±0.377	—	—	—	—	—	—
	2	0.43359−0.47278	175	-1.675±1.208	-3.543	1.546	2.843	0.544	Accept H_0	-2.527
	3	0.47279−0.50185	175	-1.074±1.761	-2.527	0.825	2.843	0.290	Accept H_0	-2.105
	4	0.50186−0.53508	175	-1.797±1.514	-2.105	0.204	2.843	0.072	Accept H_0	-2.083
	5	0.53509−0.57406	175	-3.969±1.258	-2.083	1.499	2.843	0.527	Accept H_0	-3.077
	6	0.57407−0.62397	175	-2.201±0.921	-3.077	0.952	2.843	0.335	Accept H_0	-2.784
	7	0.62398−0.68130	175	-3.099±0.800	-2.784	0.394	2.843	0.139	Accept H_0	-2.828
	8	0.68131−0.77611	175	-3.219±0.533	-2.828	0.734	2.843	0.258	Accept H_0	-2.929
	9	0.77612−0.94936	175	-3.370±0.309	-2.929	1.426	2.843	0.502	Accept H_0	-3.150
	10	0.94937−1.72354	201	-2.543±0.058	-3.150	10.426	2.838	3.674	Reject H_0	-0.919

Notes: n represents the number of non-overlapping subsets and $\log(P)$ is the period range in each subset. N and $\hat{\beta}$ represent the number of stars and slope of linear regression in each subset, respectively. β_0 and β_w represent the initial and updated testimator after each hypothesis testing. $|t_{obs}|$ is estimated using equation 6 and t_c represents the theoretical t-value for confidence level of more than 95%. k is the probability of initial guess of the testimator being true and leads to the decision of acceptance/rejection.

Table 3. Results of the Davies test on "simulated" P-L relations.

Band	N	$\log(P_b)$	σ_{P_b}	$b_{\rm low}$	$\sigma_{b_{\rm low}}$	$b_{\rm up}$	$\sigma_{b_{\rm up}}$	$c_{\rm low}$	$c_{\rm up}$	p(D)
V_L	1776	0.832	0.366	-2.739	0.094	-2.677	0.098	-1.471	-1.522	0.958
V_{NL}	1776	0.868	0.044	-3.004	0.085	-2.448	0.109	-1.318	-1.800	0.000

Notes: For the Davis test, $b_{\rm low}$ refers to the slope for $P < P_b$ and $\sigma_{b_{\rm low}}$ is the uncertainty in the slope. Similarly, $b_{\rm up}$ refers to the slope for $P > P_b$ and $\sigma_{b_{\rm up}}$ is the associated uncertainty. $c_{\rm low}$ and $c_{\rm up}$ represent the intercept of the linear fit for $P < P_b$ and $P > P_b$, respectively. $p(D)$ represents the probability of acceptance of null hypothesis i.e. linear relation.

mode Cepheids with periods below 2.5 days because of the small sample size. The results of statistical tests applied to these FU and FO mode Cepheid datasets are discussed in following subsections.

4.3 Fundamental-mode Cepheids

In Bhardwaj et al. (2014), we found a significant change in the slope of the P-C relation at maximum and minimum light for FU mode Cepheids with periods greater than 10 days in the LMC. The non-linearity in the optical band P-L and P-C relations at a period of 10 days for Cepheid variables is discussed extensively in previous studies (see references in §1). Ngeow et al. (2009) used F-test to determine non-linearity in P-L relations for FU mode Cepheids using OGLE-III data. We revisit the breaks at 10 days in P-L relation observed by Ngeow et al. (2009) with more test-statistics and determine their statistical significance in order to compare with our new near-infrared data. The results of the F-test and the random walk method for FU mode Cepheids at multiple bands are presented in Table 4. The results of the testimator and the Davis test are given in Table A1 and Table 5, respectively.

The optical and near-infrared band P-L and P-W relations for FU mode Cepheids are presented in Fig. 2. Visual inspection of the V- and I-band P-L relations reveals a small variation in the slope. The results of test statistics are as follows:

- The optical band P-L relations are non-linear at 10 days according to the F-test, testimator and the Davis test.
- Since the optical band P-L relations have higher dispersion with consequently larger residuals at longer periods using a single regression line, the random walk does not provide evidence to support a non-linearity at the 90-95% significance level. The random walk gives a p-value of 0.168 and 0.128 for V- and I-band P-L relations, respectively.
- As the F-test, Davis test and the testimator result in a non-linear relation, we consider the V- and I-band P-L relations to be non-linear.
- The F-test and the Davis test also indicate that the optical-band P-W relation is nonlinear, although the deviation from a single slope is considerably smaller.

Table 4. Results of the F and random walk test on P-L, P-W and P-C relations for FU mode Cepheids in the LMC, to check the period breaks at 10 days. The optical band results are for OGLE-III sample. The JHK_s band results are for the near-infrared counterparts of OGLE-III stars. The meaning of each column header is discussed in Table 1.

Y	b_{all}	σ_{all}	N_{all}	b_S	σ_S	N_S	b_L	σ_L	N_L	F	$p(F)$	$p(R)$
V	-2.679±0.023	0.177	1546	-2.743±0.032	0.172	1440	-2.285±0.185	0.232	106	6.404	0.002	0.168
I	-2.928±0.016	0.121	1537	-2.973±0.022	0.117	1433	-2.628±0.127	0.161	104	7.374	0.001	0.128
J	-3.147±0.016	0.115	774	-3.118±0.031	0.109	665	-3.336±0.071	0.144	109	5.504	0.004	0.037
H	-3.158±0.013	0.095	774	-3.106±0.026	0.090	665	-3.320±0.060	0.120	109	7.219	0.001	0.044
K_s	-3.221±0.011	0.084	774	-3.192±0.022	0.079	665	-3.361±0.055	0.111	109	5.994	0.003	0.076
$W_{V,I}$	-3.312±0.010	0.074	1567	-3.335±0.013	0.071	1469	-3.262±0.093	0.107	98	3.040	0.048	0.293
$W_{J,H}$	-3.152±0.014	0.107	774	-3.086±0.029	0.107	665	-3.297±0.055	0.106	109	6.211	0.002	0.085
W_{J,K_s}	-3.273±0.010	0.077	774	-3.242±0.020	0.074	665	-3.378±0.048	0.095	109	4.634	0.010	0.211
W_{H,K_s}	-3.361±0.013	0.100	774	-3.356±0.026	0.099	665	-3.436±0.052	0.107	109	1.240	0.290	0.627
$W_{V,J}$	-3.300±0.013	0.092	697	-3.289±0.025	0.089	590	-3.472±0.052	0.106	107	7.456	0.001	0.193
$W_{V,H}$	-3.236±0.013	0.094	699	-3.225±0.025	0.089	592	-3.393±0.058	0.116	107	5.681	0.004	0.158
W_{V,K_s}	-3.284±0.010	0.072	698	-3.263±0.019	0.068	592	-3.381±0.045	0.090	106	4.015	0.018	0.225
$W_{I,J}$	-3.288±0.016	0.114	702	-3.279±0.031	0.110	593	-3.491±0.064	0.127	109	6.719	0.001	0.151
$W_{I,H}$	-3.225±0.012	0.087	699	-3.184±0.024	0.084	592	-3.380±0.049	0.100	107	7.645	0.001	0.076
W_{I,K_s}	-3.280±0.010	0.075	699	-3.260±0.020	0.071	593	-3.378±0.046	0.093	106	3.718	0.025	0.320
$W^H_{V,I}$	-3.247±0.010	0.076	699	-3.220±0.020	0.072	593	-3.369±0.047	0.094	106	5.763	0.003	0.095
$V-I$	0.242±0.008	0.065	1557	0.218±0.012	0.063	1453	0.398±0.067	0.081	104	6.823	0.001	0.197
$J-H$	0.002±0.006	0.042	690	-0.012±0.011	0.042	582	-0.018±0.020	0.041	108	1.387	0.251	0.461
$J-K_s$	0.073±0.006	0.046	684	0.068±0.013	0.045	577	0.022±0.023	0.047	107	3.153	0.053	0.603
$H-K_s$	0.072±0.004	0.031	688	0.077±0.009	0.032	579	0.040±0.012	0.021	109	2.415	0.090	0.489
$V-J$	0.385±0.017	0.120	687	0.374±0.034	0.115	578	0.363±0.073	0.146	109	0.159	0.853	0.276
$V-H$	0.391±0.020	0.141	686	0.373±0.039	0.134	577	0.347±0.086	0.174	109	0.365	0.695	0.204
$V-K_s$	0.459±0.020	0.142	685	0.449±0.040	0.135	577	0.397±0.087	0.176	108	0.465	0.628	0.459
$I-J$	0.156±0.009	0.067	690	0.150±0.020	0.066	581	0.172±0.037	0.075	109	0.154	0.857	0.089
$I-H$	0.162±0.012	0.085	687	0.147±0.024	0.082	578	0.156±0.049	0.099	109	0.287	0.751	0.176
$I-K_s$	0.233±0.012	0.087	687	0.229±0.025	0.083	579	0.202±0.051	0.102	108	0.304	0.738	0.163

Table 5. Results from Davies test on P-L, P-W and P-C relations for FU mode Cepheids. The meaning of each column header is discussed in Table 3.

	N	$\log(P_b)$	σ_{P_b}	$b_{\rm low}$	$\sigma_{b_{\rm low}}$	$b_{\rm up}$	$\sigma_{b_{\rm up}}$	$c_{\rm low}$	$c_{\rm up}$	$p(D)$
V	1546	1.004	0.076	-2.748	0.064	-2.323	0.292	17.30	16.87	0.006
I	1537	1.014	0.069	-2.977	0.044	-2.655	0.204	16.76	16.43	0.003
J	774	1.262	0.089	-3.087	0.044	-3.473	0.266	16.31	16.79	0.003
H	774	1.259	0.075	-3.093	0.036	-3.469	0.217	15.95	16.42	0.000
K_s	774	1.275	0.081	-3.177	0.032	-3.496	0.204	15.96	16.37	0.001
$W_{V,I}$	1567	0.899	0.101	-3.339	0.032	-3.231	0.087	15.92	15.82	0.098
$W_{J,H}$	774	1.256	0.086	-3.103	0.039	-3.465	0.236	15.37	15.83	0.001
W_{J,K_s}	774	1.275	0.088	-3.237	0.028	-3.502	0.185	15.73	16.06	0.002
W_{H,K_s}	774	1.314	0.138	-3.335	0.036	-3.543	0.251	15.98	16.26	0.292
$W_{V,J}$	697	1.261	0.096	-3.263	0.034	-3.537	0.200	15.96	16.30	0.005
$W_{V,H}$	699	1.253	0.107	-3.201	0.036	-3.462	0.214	16.09	16.42	0.012
W_{V,K_s}	698	1.247	0.109	-3.255	0.028	-3.446	0.159	15.82	16.05	0.016
$W_{I,J}$	702	1.313	0.085	-3.246	0.041	-3.633	0.286	15.98	16.49	0.009
$W_{I,H}$	699	1.250	0.081	-3.177	0.032	-3.494	0.191	15.66	16.06	0.000
W_{I,K_s}	699	1.251	0.113	-3.251	0.028	-3.446	0.169	15.80	16.05	0.020
$W^H_{V,I}$	699	1.248	0.095	-3.214	0.028	-3.443	0.165	15.76	16.05	0.004
$V-I$	1557	1.038	0.069	0.218	0.022	0.400	0.127	0.554	0.365	0.005
$J-H$	698	0.471	0.035	0.248	0.434	0.001	0.012	0.243	0.360	0.453
$J-K_s$	684	0.466	0.034	0.378	0.540	0.076	0.013	0.209	0.350	0.484
$H-K_s$	688	1.208	0.141	0.083	0.012	0.026	0.055	-0.014	0.054	0.087
$V-J$	687	0.516	0.049	0.761	0.603	0.355	0.041	0.805	1.015	0.552
$V-H$	686	0.523	0.054	0.784	0.644	0.361	0.047	1.150	1.371	0.554
$V-K_s$	685	0.463	0.029	1.613	1.882	0.443	0.043	0.810	1.352	0.618
$I-J$	690	0.540	0.075	0.279	0.262	0.135	0.025	0.376	0.454	0.868
$I-H$	687	0.529	0.058	0.373	0.353	0.143	0.029	0.685	0.807	0.556
$I-K_s$	687	0.481	0.038	0.694	0.776	0.222	0.027	0.564	0.791	0.592

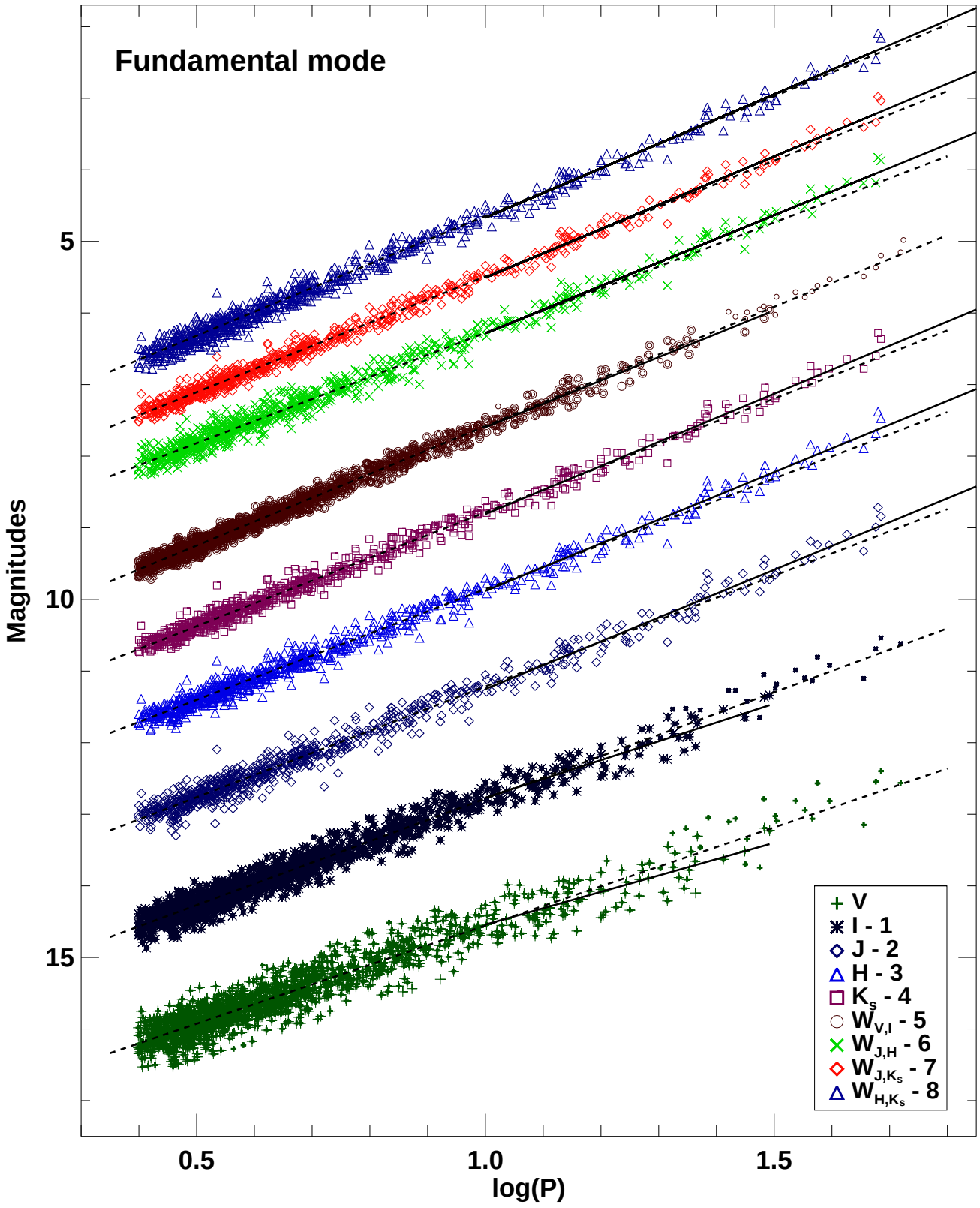

Figure 2. Optical and near-infrared P-L and P-W relations for LMC FU mode Cepheids. The dashed/solid lines represent the best fit regression for Cepheids with periods below and above 10 days. The smaller symbol for longer period Cepheids at optical bands represents stars from OGLE-III-SS.

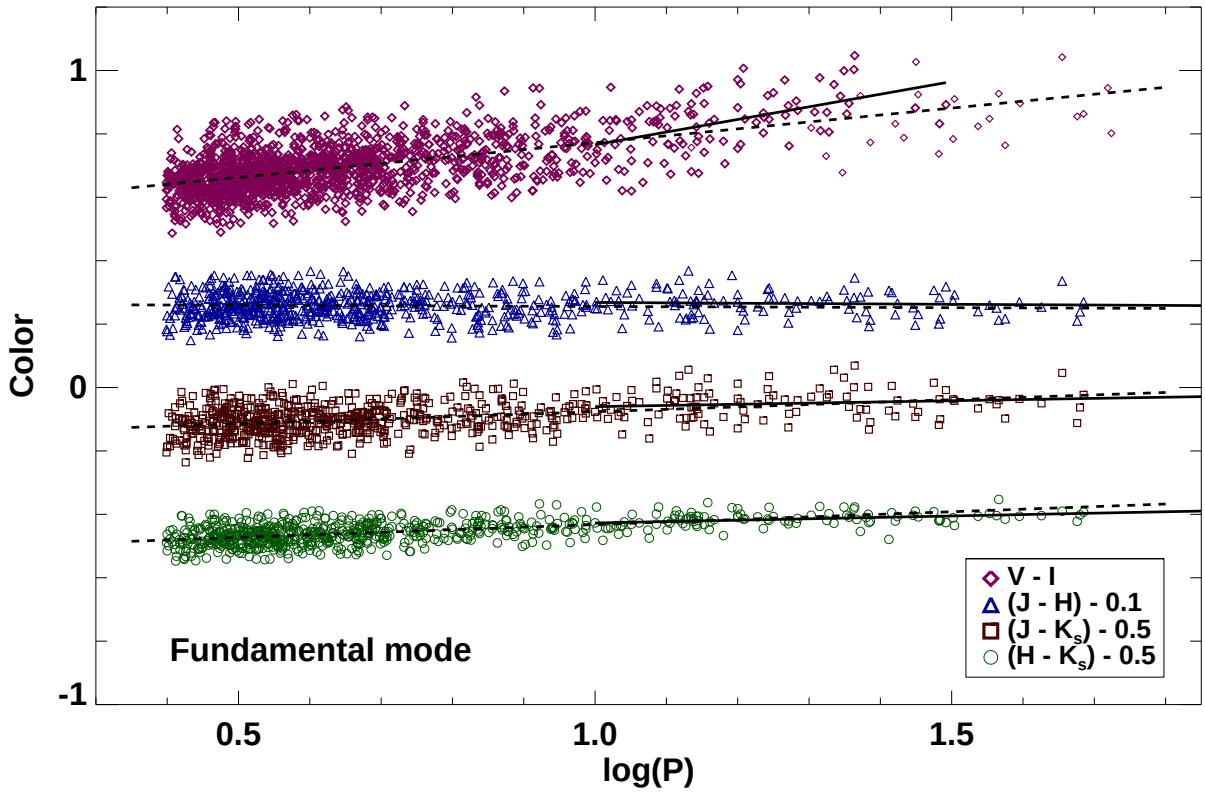

Figure 3. Optical and near-infrared P-C relations for LMC FU mode Cepheids. The dashed/solid lines represent the best fit regression for Cepheids with periods below and above 10 days. The smaller symbol for longer period Cepheids at optical bands represents stars from OGLE-III-SS.

Table 6. Results of the F and random walk test on optical bands P-L, P-W and P-C relations for FU mode Cepheids in OGLE-III-SS sample, to check period breaks at 10 days. The meaning of each column header is discussed in Table 1.

Y	b_{all}	σ_{all}	N_{all}	b_S	σ_S	N_S	b_L	σ_L	N_L	F	$p(F)$	$p(R)$
V	-2.733±0.021	0.179	1569	-2.764±0.032	0.172	1441	-2.829±0.123	0.251	128	1.577	0.207	0.449
I	-2.964±0.014	0.122	1560	-2.979±0.022	0.118	1436	-3.020±0.083	0.168	124	0.893	0.409	0.450
$W_{V,I}$	-3.330±0.009	0.074	1590	-3.335±0.013	0.071	1470	-3.407±0.051	0.105	120	2.746	0.064	0.448
$V-I$	0.228±0.007	0.065	1580	0.218±0.012	0.063	1453	0.194±0.042	0.087	127	1.285	0.277	0.675

• Similarly, the P-C relation shown in Fig. 3, exhibit a significant non-linearity at 10 days in the optical bands.

We note, however, that these results do not hold if we use the OGLE-III-SS data set. The results for the F-test and random walk are presented in Table 6, while Table A2 and Table 7 present the results of the testimator and the Davis test, respectively. All the test statistics rule out the possibility of a break at 10 days in the P-L relations. We note that while adding the longer-period variables increases the sample size relative to OGLE-III, it also results in increased dispersion for longer period range P-L relations. Similarly, the P-C relation using OGLE-III-SS data also does not provide any evidence of a non-linearity at 10 days, according to all the test statistics. Since we observed a non-linearity in the P-C relations at maximum and minimum light for this sample in Bhardwaj et al. (2014), we plan to look into the characteristics of the multi-phase P-L and P-C relations before reaching any further conclusions. We present the V-band P-L relation at two phases of pulsation using OGLE-III-SS data set, displayed in Fig. 4. All the test statistics provide evidence of a significantly non-linear P-L relation at these phases. A detailed statistical analysis of these relation as a function of phase will be presented in a subsequent study. However, the P-W relation for the OGLE-III-SS sample does provide evidence of a marginally significant non-linearity using the F-test (p-value $\sim$ 0.06), the Davis test (p-value $\sim$ 0.08) and the testimator. We note from Table 6 that the dispersion in this P-W relation is less (only 0.074 mag), compared to 0.179 and 0.122 for the V- and I-band P-L relations.

We extend our analysis to test for the first time the possibility of non-linearities in the near-infrared P-L and

Table 7. Results from Davies test on P-L, P-W and P-C relations for Cepheids in the OGLE-III-SS sample. The meaning of each column header is discussed in Table 3.

Band	N	$\log(P_b)$	σ_{P_b}	$b_{\rm low}$	$\sigma_{b_{\rm low}}$	$b_{\rm up}$	$\sigma_{b_{\rm up}}$	$c_{\rm low}$	$c_{\rm up}$	$p(D)$
V	1569	1.308	0.144	-2.711	0.048	-3.069	0.514	17.28	17.750	0.494
I	1560	1.354	0.143	-2.950	0.032	-3.253	0.460	16.740	17.150	0.484
$W_{V,I}$	1590	1.249	0.159	-3.318	0.021	-3.453	0.171	15.910	16.070	0.081
$V-I$	1580	1.369	0.129	0.237	0.017	0.029	0.264	0.543	0.827	0.129

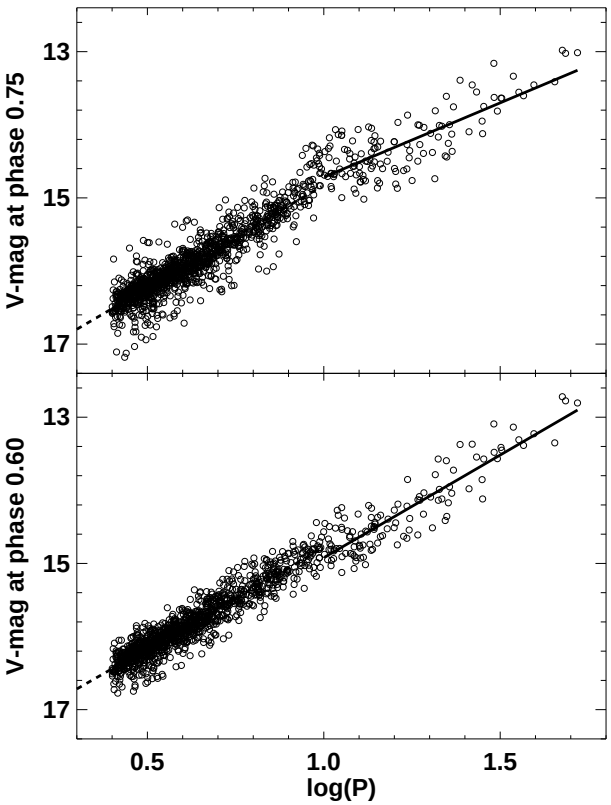

Figure 4. The V-band P-L relations for LMC FU mode Cepheids using OGLE-III-SS data. The dashed/solid lines represent the best fit regression for Cepheids with periods below and above 10 days.

P-W relations derived using time-series observations. The results of the test statistics are as follows:

- A small but statistically significant change in the slope for longer period Cepheids is observed in the near-infrared P-L relations, according to all four test statistics.
- The Davis test suggests a break around $\log(P) \sim 1.25$-1.30 in the near-infrared P-L relations. Similarly, Bhardwaj et al. (2015b) observed a distinct variation in the Fourier amplitude parameters for longer wavelengths as compared to optical bands around a period of 20 days. This indicates that the observed non-linearities in these relations are in fact associated with sharp variations in light curve structure as discussed in Bhardwaj et al. (2014). It is a very interesting result relating changes in light curve parameters with breaks in P-L and/or P-C relations, i.e. physical parameters.
- In the case of the near-infrared P-W relations, $W_{J,H}$ and W_{J,K_s} are found to be non-linear at $\log(P) \sim 1.25$, according to most test statistics.
- However, W_{H,K_s} is linear according to the F, random walk and Davis tests. As the longer wavelengths are expected to be less sensitive to metallicity and extinction, this linearity may be very useful in distance scale applications. Further, this may also indicate the effect of metallicities on the linearity of a P-L relation and will be subsequently investigated as a function of pulsation phase.
- We also note that the $W^H_{V,I}$ relation, which is commonly used (Riess et al. 2009, 2011) for calibrating the distances to SNe Ia host galaxies and determining the value of the Hubble constant, H_0, is non-linear according to all four test statistics. Again, the Davis test provides evidence of a significant change in the slope at $\log(P) \sim 1.248$.
- The optical-near-infrared P-W relations are also non-linear according to most test statistics, resulting in the adopted non-linear relation for all combinations.
- The P-C relation at near-infrared wavelengths are shown in Fig. 3 together with the optical band P-C relation. However, these relations do not provide any evidence of possible non-linearity at 10 days and suggest that the temperature fluctuations are less dominant at these wavelengths.
- We note that the multi-wavelength LMC P-L relations are found to be non-linear in this study but the SMC P-L relations are linear at 10 days (Ngeow et al. 2015).

4.4 First-overtone mode Cepheids

Non-linearity in the P-L and P-C relations is discussed in detail in the literature for FU mode Cepheids. In Bhardwaj et al. (2014), we also found significant breaks in the P-C and A-C relations at 2.5 days for FO mode Cepheids in the Magellanic Clouds at the phases of maximum and minimum light. We extend that work to see if these breaks exist in the P-L, P-W and P-C relations at mean light in multiple bands. The results of the F-test and the random-walk method are summarized in Table 8, while Table A3 and Table 9 present the results for the testimator and the Davis test, respectively.

The optical and near-infrared band P-L and P-W relations for FO mode Cepheids are presented in Fig. 5. Both optical band P-L relations present evidence of a clear non-linearity around 2.5 days based on all four test statistics. The P-W relation is also consistent with a break at the same period using all test statistics. It is important to note that the Davis test suggests a break at $\log(P) = 0.45$ ($P \sim 2.8$) days

Table 8. Results for F test and random walk on P-L, P-W and P-C relations for FO mode Cepheids in LMC, to check period breaks at 2.5 days. The meaning of each column header is discussed in Table 1.

Y	b_{all}	σ_{all}	N_{all}	b_S	σ_S	N_S	b_L	σ_L	N_L	F	$p(F)$	$p(R)$
V	-3.299±0.029	0.182	1084	-3.410±0.045	0.187	802	-2.688±0.108	0.155	282	16.080	0.000	0.000
I	-3.354±0.021	0.129	1084	-3.430±0.032	0.132	802	-2.894±0.078	0.112	282	17.231	0.000	0.000
J	-3.336±0.038	0.114	474	-3.455±0.064	0.117	348	-3.107±0.103	0.102	126	3.166	0.043	0.122
H	-3.258±0.029	0.092	474	-3.322±0.049	0.097	348	-3.117±0.075	0.075	126	2.000	0.136	0.284
K_s	-3.276±0.025	0.081	474	-3.303±0.042	0.087	348	-3.179±0.062	0.062	126	0.979	0.376	0.277
$W_{V,I}$	-3.466±0.011	0.069	1075	-3.517±0.017	0.070	790	-3.359±0.045	0.066	285	9.145	0.000	0.000
$W_{J,H}$	-3.076±0.035	0.119	474	-3.099±0.061	0.130	348	-3.141±0.093	0.084	126	0.388	0.678	0.505
W_{J,K_s}	-3.216±0.024	0.082	474	-3.194±0.042	0.089	348	-3.230±0.060	0.062	126	0.269	0.764	0.324
W_{H,K_s}	-3.319±0.035	0.119	474	-3.264±0.060	0.130	348	-3.295±0.088	0.089	126	0.939	0.392	0.026
$W_{V,J}$	-3.436±0.029	0.095	422	-3.526±0.049	0.099	301	-3.288±0.084	0.082	121	3.522	0.030	0.109
$W_{V,H}$	-3.391±0.028	0.093	421	-3.463±0.046	0.096	300	-3.241±0.082	0.082	121	2.904	0.056	0.179
W_{V,K_s}	-3.293±0.021	0.071	421	-3.322±0.037	0.078	300	-3.252±0.053	0.053	121	0.622	0.537	0.488
$W_{I,J}$	-3.433±0.036	0.118	420	-3.519±0.061	0.124	299	-3.291±0.106	0.101	121	2.052	0.130	0.249
$W_{I,H}$	-3.254±0.026	0.086	422	-3.325±0.046	0.095	301	-3.221±0.061	0.062	121	2.218	0.110	0.174
W_{I,K_s}	-3.280±0.022	0.074	420	-3.299±0.039	0.081	299	-3.249±0.055	0.056	121	0.275	0.760	0.404
$W^H_{V,I}$	-3.314±0.021	0.070	421	-3.394±0.037	0.076	300	-3.232±0.053	0.055	121	4.580	0.011	0.049
$V-I$	0.064±0.010	0.064	1086	0.033±0.016	0.066	803	0.269±0.038	0.054	283	13.344	0.000	0.002
$J-H$	-0.113±0.015	0.050	408	-0.139±0.026	0.054	293	-0.026±0.039	0.039	115	2.150	0.118	0.200
$J-K_s$	-0.089±0.017	0.057	408	-0.139±0.028	0.058	291	0.048±0.052	0.052	117	4.851	0.008	0.169
$H-K_s$	0.035±0.013	0.045	416	0.013±0.024	0.048	295	0.046±0.035	0.036	121	0.777	0.460	0.043
$V-J$	0.110±0.038	0.126	407	0.064±0.062	0.130	290	0.353±0.116	0.112	117	2.183	0.114	0.121
$V-H$	-0.024±0.042	0.142	404	-0.091±0.070	0.147	288	0.316±0.123	0.122	116	3.495	0.031	0.090
$V-K_s$	-0.010±0.045	0.152	406	-0.107±0.075	0.157	290	0.359±0.134	0.135	116	3.947	0.020	0.114
$I-J$	0.062±0.022	0.074	404	0.045±0.036	0.075	285	0.163±0.070	0.068	119	1.090	0.337	0.378
$I-H$	-0.083±0.026	0.088	403	-0.124±0.044	0.092	287	0.132±0.072	0.071	116	3.636	0.027	0.024
$I-K_s$	-0.072±0.028	0.094	404	-0.143±0.046	0.097	288	0.174±0.082	0.082	116	4.860	0.008	0.043

Table 9. Results from Davies test on P-L, P-W and P-C relations for FO mode Cepheids. The meaning of each column header is discussed in Table 3.

	N	$\log(P_b)$	σ_{P_b}	$b_{\rm low}$	$\sigma_{b_{\rm low}}$	$b_{\rm up}$	$\sigma_{b_{\rm up}}$	$c_{\rm low}$	$c_{\rm up}$	$p(D)$
V	1084	0.446	0.030	-3.468	0.084	-2.684	0.314	16.90	16.55	0.000
I	1084	0.449	0.030	-3.474	0.058	-2.920	0.229	16.32	16.07	0.000
J	474	0.427	0.064	-3.484	0.116	-3.104	0.290	15.87	15.71	0.059
H	474	0.422	0.075	-3.332	0.087	-3.094	0.212	15.49	15.39	0.156
K_s	474	0.019	0.086	-2.860	0.820	-3.301	0.055	15.46	15.47	0.735
$W_{V,I}$	1075	0.381	0.039	-3.533	0.036	-3.340	0.082	15.43	15.35	0.000
$W_{J,H}$	474	0.149	0.106	-3.317	0.427	-3.026	0.096	14.90	14.86	0.510
W_{J,K_s}	474	0.070	0.050	-2.761	0.468	-3.257	0.058	15.17	15.21	0.045
W_{H,K_s}	474	0.066	0.030	-2.247	0.664	-3.410	0.083	15.38	15.45	0.000
$W_{V,J}$	422	0.391	0.068	-3.522	0.094	-3.278	0.177	15.49	15.40	0.091
$W_{V,H}$	421	0.409	0.074	-3.462	0.086	-3.237	0.188	15.62	15.53	0.172
W_{V,K_s}	421	0.014	0.066	-2.815	0.728	-3.314	0.047	15.29	15.30	0.261
$W_{I,J}$	420	0.394	0.089	-3.514	0.116	-3.281	0.224	15.52	15.43	0.323
$W_{I,H}$	422	0.210	0.091	-3.406	0.214	-3.197	0.079	15.19	15.15	0.257
W_{I,K_s}	420	0.072	0.058	-2.929	0.409	-3.313	0.055	15.27	15.29	0.134
$W^{H_{V,I}}$	421	0.373	0.060	-3.386	0.071	-3.201	0.114	15.29	15.22	0.046
$V-I$	1086	0.473	0.032	0.014	0.028	0.298	0.134	0.581	0.447	0.000
$J-H$	408	0.417	0.077	-0.147	0.048	-0.022	0.111	0.373	0.321	0.216
$J-K_s$	408	0.460	0.042	-0.157	0.046	0.124	0.153	0.398	0.269	0.000
$H-K_s$	416	0.151	0.044	-0.171	0.159	0.078	0.035	0.033	-0.005	0.002
$V-J$	407	0.465	0.099	0.047	0.110	0.350	0.402	1.049	0.908	0.432
$V-H$	404	0.455	0.079	-0.123	0.121	0.274	0.411	1.425	1.244	0.191
$V-K_s$	406	0.456	0.065	-0.136	0.127	0.385	0.440	1.449	1.212	0.043
$I-J$	404	0.280	0.186	0.091	0.124	0.021	0.083	0.448	0.468	1.000
$I-H$	403	0.455	0.092	-0.134	0.074	0.074	0.252	0.837	0.742	0.384
$I-K_s$	404	0.453	0.060	-0.157	0.080	0.186	0.269	0.864	0.709	0.024

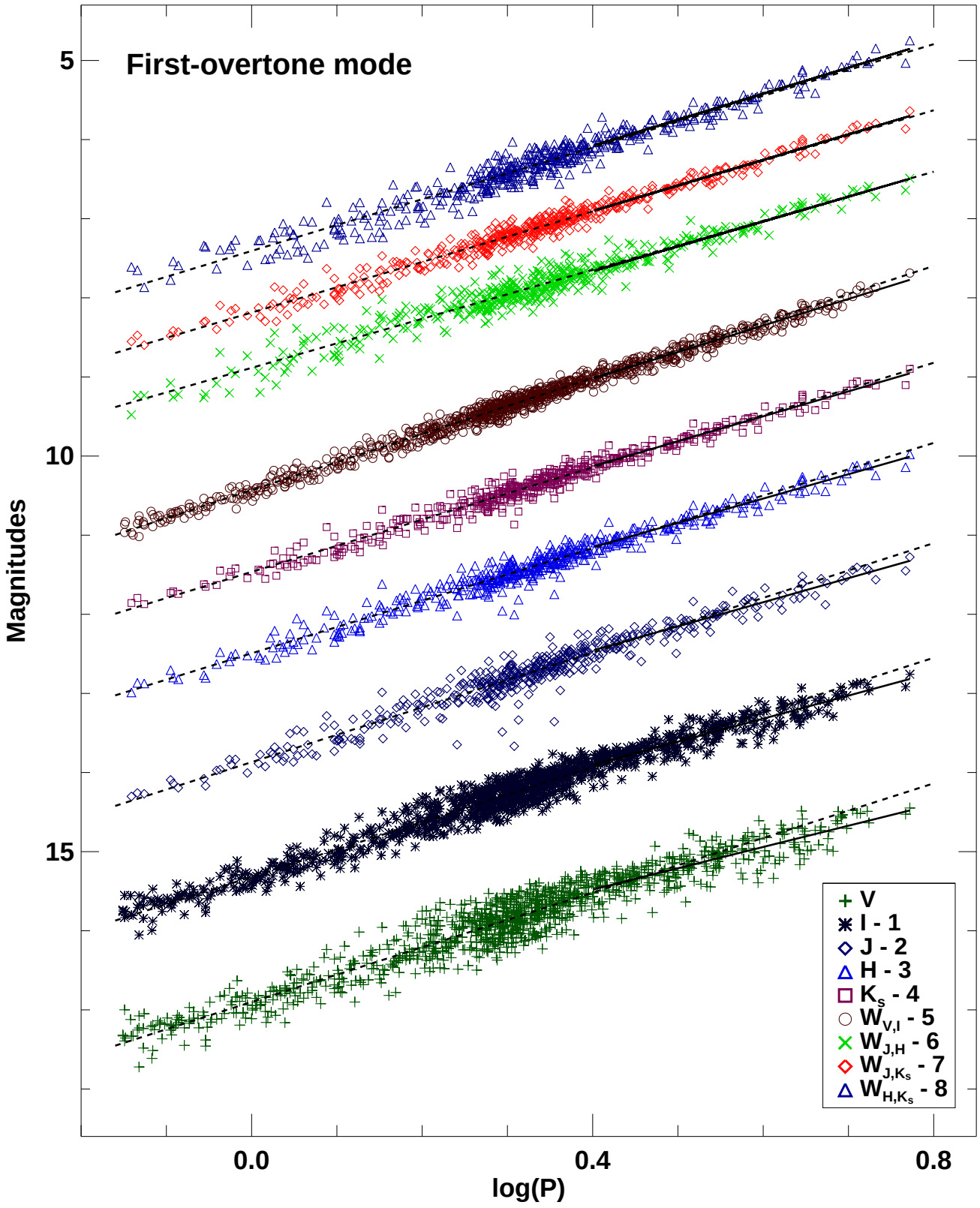

Figure 5. Optical and near-infrared P-L and P-W relations for LMC FO mode Cepheids. The dashed/solid lines represent the best fit regression for Cepheids with periods below and above 2.5 days.

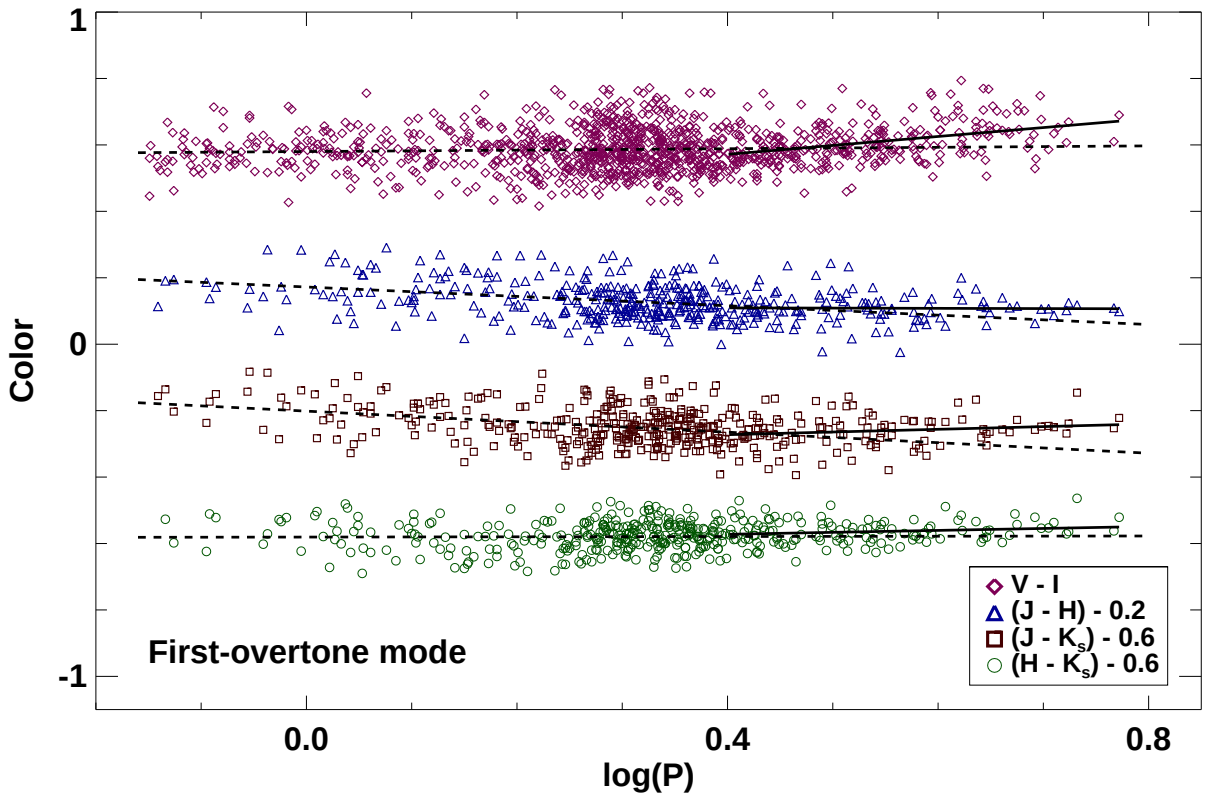

Figure 6. Optical and near-infrared P-C relations for LMC FO mode Cepheids. The dashed/solid lines represent the best fit regression for Cepheids with periods below and above 10 days.

in P-L relations. Similarly, the testimator also provides evidence of a break in period bin covering range from 2.5 days to 5 days. A further trend can be seen in optical P-L relations at 0.6 days but there are not enough data points so we discard any such non-linearity and these stars are not shown in Fig. 5.

At near-infrared wavelengths, we find a small but significant change in the slope of the J-band P-L relation using the F and the testimator tests, but the random walk and Davis test do not find evidence to support a non-linear relation. However, all the tests except the testimator, provide evidence of a linear P-L relation in H- & K_s. So for FO mode stars, evidence for a non-linearity diminishes with increasing wavelength. Similarly, in the case of P-W relations, the F-test, Davis test and the testimator results in a linear relation in W_{H,K_s}. All four test statistics result in a non-linear $W^H_{V,I}$ relation. Therefore, both FU and FO mode Cepheid follow a linear P-W relation in W_{H,K_s} but a non-linear relation in $W^H_{V,I}$. The optical and near-infrared combinations of P-W relations provide mixed results depending on the test statistics under consideration and result in adopted linear relations for most of the combinations. The optical and near-infrared bands P-C relations for FO mode Cepheids are shown in Fig. 6. All tests yield significant detection of non-linearity at 2.5 days in optical bands. At near-infrared wavelengths, only $(J-K_s)$ color provide evidence of a change in slope of P-C relation. The mixed optical-infrared band colors result in a non-linear P-C relation for most combinations. The test results for all FU and FO mode Cepheids are summarized in Table 10.

4.5 Robustness of the test-statistics

As discussed in Section 3, the F-distribution requires the independent and identically distributed random variables and works under the assumption of homoskedasticity and normality of residuals. In order to validate our F-test results, we need to investigate if our data follows these assumptions. Since observations of each Cepheid are independent of other observations, the assumption of variables being independent and identically distributed is satisfied. Fig. 7 displays the residuals of linear regression to V- and J-band P-L relations for FU and FO mode Cepheids in the LMC. We do not see any significant trend in the residuals, that can violate the assumption of homoskedasticity. Further, the mean residuals for all these relations are consistent with zero and therefore, the homoskedasticity assumption holds well for our data.

However, we see some trend on the extreme ends in the quantile-quantile (q-q) plots for the P-L, P-W and P-C relations. These plots are generally used to describe the normality of residuals. We have displayed the q-q plot for V- and J-band P-L relations for FU and FO mode Cepheids in Fig. 8. Even though the majority of residual quantiles fall on the $y = x$ line, there are some outliers on the extreme ends. In order to ensure that these outliers do not belong to only

Table 10. Results of non-linearities in P-L, P-W and P-C relations for FU and FO mode Cepheids in LMC at multiple wavelengths.

OGLE-III + CPAPIR										
	FU					**FO**				
	FT	RW	TM	DT	AD	FT	RW	TM	DT	AD
V_L	✘	✘	✘	✘	✘	–	–	–	–	–
V_{NL}	✔	✔	✔	✔	✔	–	–	–	–	–
V	✔	✘	✔	✔	✔	✔	✔	✔	✔	✔
I	✔	✘	✔	✔	✔	✔	✔	✔	✔	✔
J	✔	✔	✔	✔	✔	✔	✘	✔	✘	✔
H	✔	✔	✔	✔	✔	✘	✘	✔	✘	✘
K_s	✔	✔	✔	✔	✔	✘	✘	✔	✘	✘
$W_{V,I}$	✔	✘	✔	✘	✔	✔	✔	✔	✔	✔
$W_{J,H}$	✔	✔	✔	✔	✔	✘	✘	✔	✘	✘
W_{J,K_s}	✔	✘	✔	✔	✔	✘	✘	✘	✘	✘
W_{H,K_s}	✘	✘	✔	✘	✘	✘	✔	✘	✘	✘
$W_{V,J}$	✔	✘	✘	✔	✔	✔	✘	✔	✘	✔
$W_{V,H}$	✔	✘	✘	✔	✔	✘	✘	✔	✘	✘
W_{V,K_s}	✔	✘	✔	✔	✔	✘	✘	✘	✘	✘
$W_{I,J}$	✔	✘	✘	✔	✔	✘	✘	✘	✘	✘
$W_{I,H}$	✔	✔	✘	✔	✔	✘	✘	✘	✘	✘
W_{I,K_s}	✔	✘	✔	✔	✔	✘	✘	✘	✘	✘
$W^H_{V,I}$	✔	✔	✔	✔	✔	✔	✔	✔	✔	✔
$V-I$	✔	✘	✘	✔	✔	✔	✔	✔	✔	✔
$J-H$	✘	✘	✘	✘	✘	✘	✘	✘	✘	✘
$J-K_s$	✘	✘	✘	✘	✘	✔	✘	✔	✔	✔
$H-K_s$	✘	✘	✘	✘	✘	✘	✔	✘	✘	✘
$V-J$	✘	✘	✔	✘	✘	✘	✘	✔	✘	✘
$V-H$	✘	✘	✘	✘	✘	✔	✔	✔	✘	✔
$V-K_s$	✘	✘	✘	✘	✘	✔	✘	✔	✔	✔
$I-J$	✘	✔	✘	✘	✘	✘	✘	✘	✘	✘
$I-H$	✘	✘	✘	✘	✘	✔	✔	✔	✘	✔
$I-K_s$	✘	✘	✘	✘	✘	✔	✔	✔	✔	✔
OGLE-III-SS										
V	✘	✘	✘	✘	✘	–	–	–	–	–
I	✘	✘	✘	✘	✘	–	–	–	–	–
$W_{V,I}$	✘	✘	✔	✘	✘	–	–	–	–	–
$V-I$	✘	✘	✘	✘	✘	–	–	–	–	–

(i) For each band P-L, P-W or P-C relations, ✔/✘ represent the break/no break under each test statistics.

(ii) For the F-test, the break is accepted if F-value > 3.

(iii) For the random walk, it is accepted if $p(R) < 0.10$.

(iv) For the testimator, we accept a break if null hypothesis is rejected for the subset which includes break period.

(v) For the Davies test, we accept a break if $p(D) < 0.05$ (equation 11).

(vi) The adopted result is listed under "AD" column. The break is accepted if atleast two tests result in a '✔'.

long or short period Cepheids, we locate these outliers on the P-L plots and find that they are spread over the entire period range. Since the normality of the residuals is essential to trust the F-test results under theoretical F-distribution, we re-do our analysis without these outliers and find consistent results. Moreover, we used the following two methods to generate a theoretical F-distribution that is independent of the way residuals are distributed.

4.5.1 Permutation method

This method is similar to the random walk test. At first, we fit a single regression line and a two line fit with a break at 10 days and estimate the observed value of F-statistics (F_0) using equation 3. In order to develop theoretical F-statistic, we take the residuals of a single regression line and re-sample them without replacement. It means that each residual is considered in the new sample but at a different location selected at random. We add the new sample of residuals to the best fit linear regression to generate a pseudo dataset. Again from equation 3, we get a F-value (F_i) for the pseudo dataset. This procedure is repeated ~ 10000 times. The pro-

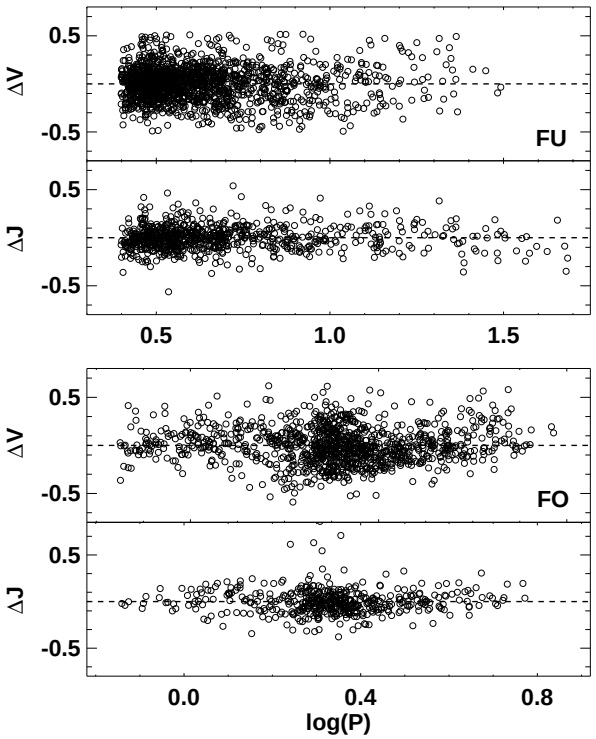

Figure 7. The residuals of a linear regression to V- and J-band P-L relation for FU and FO mode Cepheids in the LMC.

portion of the F_i, in the pseudo dataset, that are greater than the observed F_0 in the actual dataset, gives the p-value ($p_p(F)$) i.e. the probability that underlying relation is linear.

4.5.2 Bootstrap method

In this method, we follow the same procedure as in permutation method except that the residuals are re-sampled with replacement. This means that it is not necessary that each residual from single regression line is considered in the new sample. This subset consists of randomly selected residuals out of the original residuals, where each selected residual may appear more than once. Again, this sample is added to best fit linear regression to generate pseudo data and determine the F-statistic. The steps are repeated ~ 10000 times to obtain the p-value ($p_b(F)$).

The results of the permutation and bootstrap methods are listed in Table 11. The probabilities, $p_p(F)$ and $p_b(F)$ are found to be almost identical to $p(F)$ values listed in Table 4 and 8 for FU and FO mode Cepheids. This confirms that F-test results are preserved even with slight departure of residuals from normality in q-q plots.

We also test the reliability of our statistical tests with different internal dispersions around the underlying relation, whether it be linear or non-linear. We find that both the F-test and random walk methods provide correct results upto a dispersion limit of $\sigma \sim 0.5$. Further, the random walk results are also sensitive to the size of residuals. Hence, this test provides the most accurate result for a relation with least internal dispersion. The testimator is highly sensitive to the number of data points in each subset and their dispersion. After significant experimentation, we find that a nearly equal number (~ 200) of stars in each subset with 3 minimum steps of hypothesis testing is the best choice that provide accurate result even for a relatively greater dispersion. For a value of $\sigma > 0.3$, the results of the testimator do not hold as the dispersion of P-L in each subset increases significantly due to a small period range. However, the results of the Davis test hold well for even greater internal dispersions as compared to other tests. We also note that the dispersion for short and long periods range P-L relations are different and hence it is important to introduce different scatter for various period ranges and simultaneously test our results. Even though the data becomes rarer for long period Cepheids, our results hold well as most of the P-L, P-W and P-C relations have $\sigma < 0.2$. A detailed study on new tests with different dispersions for different period bins will be presented in a subsequent communication.

Table 11. Results of F-test using permutation and bootstrap methods.

	FU			**FO**		
Band	F_0	$p_b(F)$	$p_p(F)$	F_0	$p_b(F)$	$p_p(F)$
			OGLE-III			
V	6.404	0.001	0.002	16.080	0.000	0.000
I	7.374	0.001	0.001	17.231	0.000	0.000
J	5.504	0.004	0.004	3.166	0.044	0.040
H	7.219	0.001	0.001	2.000	0.135	0.140
K_s	5.994	0.003	0.004	0.979	0.383	0.377
$W_{V,I}$	3.040	0.049	0.052	9.145	0.000	0.000
$W_{J,H}$	6.211	0.002	0.002	0.388	0.683	0.679
W_{J,K_s}	4.634	0.010	0.011	0.269	0.759	0.768
W_{H,K_s}	1.240	0.287	0.286	0.939	0.396	0.381
$W_{V,J}$	7.456	0.000	0.001	3.522	0.028	0.027
$W_{V,H}$	5.681	0.003	0.004	2.904	0.056	0.054
W_{V,K_s}	4.015	0.019	0.018	0.622	0.539	0.550
$W_{I,J}$	6.719	0.002	0.001	2.052	0.129	0.125
$W_{I,H}$	7.645	0.000	0.001	2.218	0.113	0.114
W_{I,K_s}	3.718	0.023	0.027	0.275	0.758	0.762
$W^H_{V,I}$	5.763	0.003	0.004	4.580	0.011	0.010
$V-I$	6.823	0.001	0.001	13.344	0.000	0.000
$J-H$	1.387	0.250	0.251	2.150	0.119	0.113
$J-K_s$	3.153	0.042	0.043	4.851	0.008	0.008
$H-K_s$	2.415	0.090	0.090	0.777	0.460	0.466
$V-J$	0.159	0.853	0.856	2.183	0.115	0.115
$V-H$	0.365	0.696	0.700	3.495	0.032	0.031
$V-K_s$	0.465	0.632	0.624	3.947	0.018	0.021
$I-J$	0.154	0.856	0.857	1.090	0.338	0.333
$I-H$	0.287	0.750	0.752	3.636	0.025	0.028
$I-K_s$	0.304	0.742	0.745	4.860	0.009	0.008
			OGLE-III-SS			
V	1.577	0.203	0.208	—	—	—
I	0.893	0.423	0.404	—	—	—
$W_{V,I}$	2.746	0.065	0.065	—	—	—
$V-I$	1.285	0.273	0.271	—	—	—

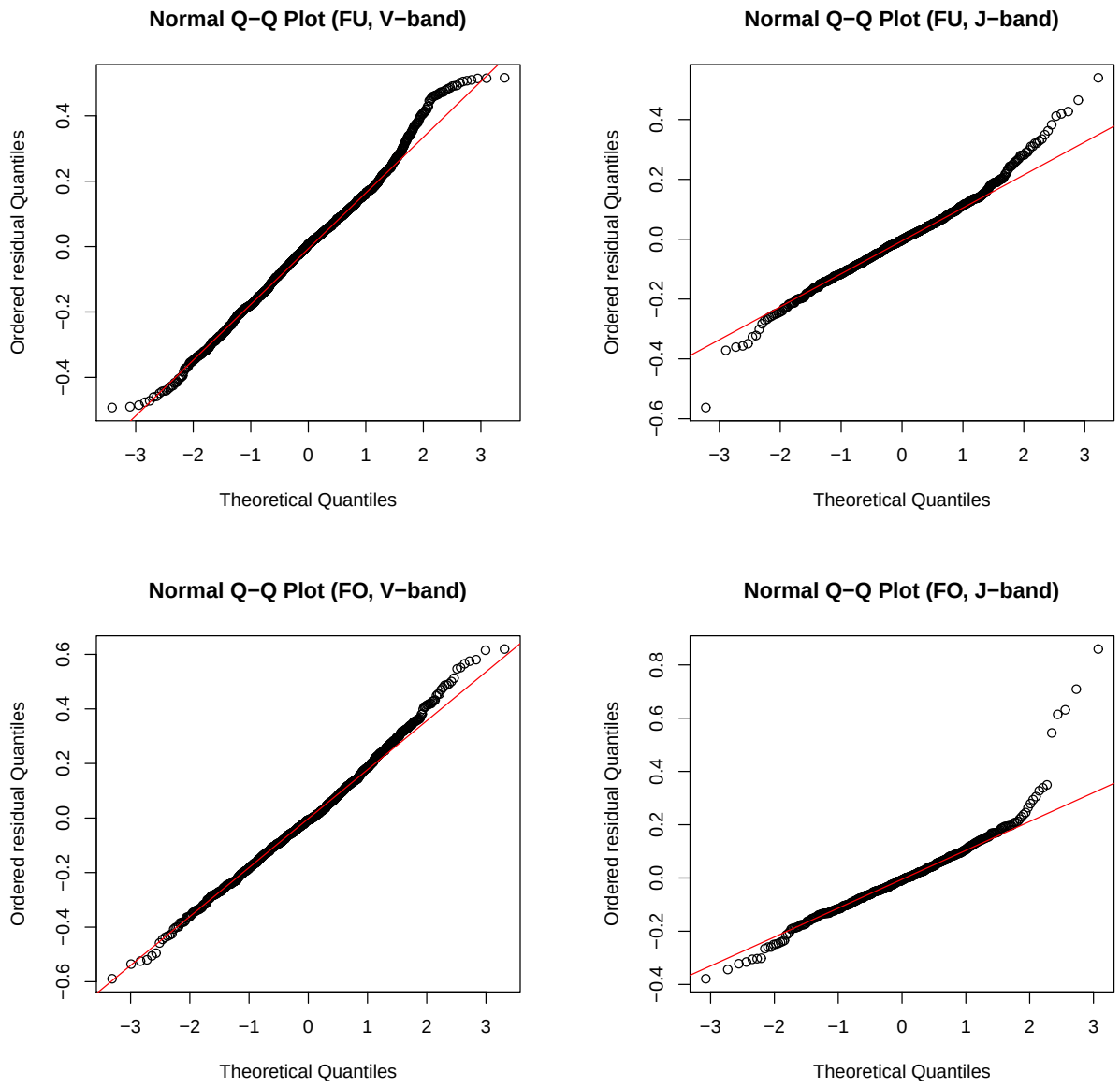

Figure 8. The quantile-quantile plot for the residuals of V- and J-band P-L relation for FU and FO mode Cepheids.

4.6 Constraints from other Cepheid hosts

The *Supernovae and H_0 for the Equation of State of dark energy* (SH0ES) project (Riess et al. 2009, 2011, hereafter, R09, R11) determined H_0 with a total uncertainty of $\sim$ 5 & 3%, respectively, using optical and near-infrared observations of Cepheids in host galaxies of type Ia supernovae (SNe Ia). The Cepheid distances to these host galaxies are estimated using the calibrated P-L relations for Cepheids in the Milky Way, LMC and NGC 4258. We note that most of the Cepheids observed in the SNe host galaxies have $P > 10$ days. Given the long-term goal of reducing the uncertainty in H_0 to $\sim 1\%$, it is important to characterize the effect of possible non-linear P-L relations on the distance scale.

In this analysis, we adopt the methodology of R09 and R11 to determine the effect of linear and non-linear P-L relations derived from a global fit to all Cepheid data, as presented in R11. Briefly, the Wesenheit magnitudes for the j^{th} Cepheid in the i^{th} SN host is defined as follows:

$$m_{w_{i,j}} = \mu_{0,i} + M_w + b_w(\log P_{i,j} - 1) + Z_w \Delta \log[O/H]_{i,j}, \quad (12)$$

where $m_{w_{i,j}}$ are the $W^H_{V,I}$ magnitudes derived in Paper II, $\mu_{0,i}$ are the distances to the SNe hosts, M_w is the calibrated Wesenheit magnitude for the Cepheid at 10 days in the calibrator galaxy, b_w is the (presumably universal) slope of the P-L relation and Z_w represents the metallicity dependence. The last three terms represent the absolute Wesenheit magnitudes for Cepheids. All four test statistics suggest that this P-W relation is non-linear and the Davis test suggests a break around 18 days. Simultaneously, for the SNe host, the V-band peak magnitude (corrected for extinction, light

curve shape, host galaxy mass, etc.) in the i^{th} host galaxy is expressed as:

$$m^0_{v,i} = \mu_{0,i} - M^0_V. \quad (13)$$

We include SNe magnitudes in our analysis to provide a tighter constraint on the global fit and also to compare with R11 results. M^0_V represents the calibrated peak magnitude of a SN Ia in the calibrator galaxy. We combine equations 12 & 13 into matrix form $y = Lq$, similar to equation 18 in R09 and solve using χ^2 minimization. We use the $m^0_{v,i}$ for the SNe Ia from the values listed in Table 3 of R11. The matrix implementation requires a covariance matrix C of measurement errors that includes photometric uncertainties in the Cepheid magnitudes and uncertainties in the SNe template fits, are adopted from R11. We estimate the values of the free parameters and their uncertainties using equation 5 from R09. We calculate the value of χ^2_{dof} and use it to re-scale the covariance matrix of errors.

We consider the following cases based on different choices of calibrator(s): (a) three galaxies (NGC 4258 + LMC + MW) (b) LMC only; (c) NGC 4258 only. We use new LMC distance of 18.493±0.0476 mag (Pietrzyński et al. 2013) and adopt the revised distance modulus for NGC 4258 of 29.404 ± 0.065 mag (Humphreys et al. 2013) to calibrate P-W relations in these galaxies. The results of the global fits for these three cases are presented in Table 12. Note that cases b & c only differ in the value and uncertainty of M_w. Column 1 represents the following variants considered in our analysis:

- **1** - The initial fit based on a sample of 510 Cepheids from R11 (using only the LMC Cepheids from Persson et al. (2004, hereafter, P04)).
- **2** - Replacing P04 LMC Cepheids in variant '1' with 710 Cepheids having $W^H_{V,I}$ magnitudes from Paper II.
- **3** - Finally, restricting the LMC sample in variant '2' to only Cepheids with $P > 10$ days.

In order to address a particular case, we will refer to the calibrator choice followed by the variant (e.g., a1 refers to the three-calibrator case with variant '1'). Our slopes are shallower for cases a1 & b1 and steeper for c1 relative to R11 (who obtained -3.21, -3.19 and -3.02, respectively), perhaps because we did not adopt a prior on the slope of the Milky Way or the LMC P-L relations. Cases a2, b2 and c2 show that the adoption of the new LMC sample results in a significant improvement of the constraint in the global slope, and the resulting value is in fact identical to the three-calibrator case of R11. It also provides a better constraint on the value of the metallicity coefficient. Lastly, cases a3, b3 and c3 show that restricting the LMC sample to long-period Cepheids only does not make any significant difference to the slope.

We recall from Table 4 that the slopes of the $W^H_{V,I}$ relations for all periods, short periods, and long periods are $b_{all} = -3.247 \pm 0.010$, $b_S = -3.220 \pm 0.020$ and $b_L = -3.369 \pm 0.047$, respectively. From Table 12, we note that the slopes of the global-fit solutions for the linear and non-linear versions (variants '2' and '3') are very consistent with the LMC-based values for b_{all} and b_S, but significantly different from b_L. In fact, the slope of the global-fit solution with LMC calibration is identical to short-period version of the solution based exclusively on LMC data.

Table 12. Results of the global fit for $W^H_{V,I}$ relation using Cepheids in SNe host galaxies.

	N	b_w	$\sigma(b_w)$	M_w	$\sigma(M_w)$	Z_w	$\sigma(Z_w)$
(a) Three calibrators							
1	510	-3.117	0.038	-5.957	0.027	-0.050	0.070
2	1165	-3.212	0.013	-5.944	0.019	0.054	0.054
3	564	-3.233	0.037	-6.015	0.026	0.030	0.066
(b) LMC as single calibrator							
1	510	-3.092	0.040	-6.029	0.053	-0.200	0.093
2	1165	-3.217	0.013	-6.062	0.039	-0.163	0.074
3	564	-3.196	0.039	-6.114	0.050	-0.169	0.090
(c) NGC 4258 as single calibrator							
1	510	-3.092	0.040	-5.954	0.032	-0.200	0.093
2	1165	-3.217	0.013	-5.908	0.023	-0.163	0.074
3	564	-3.196	0.039	-6.010	0.031	-0.169	0.090

Notes: N represents the number of stars. b_w, M_w and Z_w refer to the slope, zero-point and metallicity coefficient of the global fit solution, respectively. The corresponding columns with σ represent the uncertainties in these parameters.

The slopes obtained from a global fit to Cepheids in SH0ES galaxies using the linear and non-linear versions of the LMC P-L relations are very similar, independent of the choice of the calibrator galaxy. Therefore, we do not expect any significant impact of this parameter on the distance scale or the value of H_0, considering that the dispersion of the *HST*-based P-L relations ($\sim$ 0.3-0.4 mag) is more than three times the dispersion of the LMC P-L relation. Therefore, even a significant change in slope for the long-period P-W relation will be masked by the dispersion of the global fit and will not have any impact on distance parameters until more precise relations can be obtained with *James Webb Space Telescope*. However, our LMC P-W sample provides a better constraint on the slope of the global fit, leading to more accurate distance measurements and improved constraints on the metallicity dependence.

5 DISCUSSION AND CONCLUSIONS

In this work, we studied possible non-linearities in the Period-Luminosity, Period-Wesenheit & Period-Color relations for fundamental and first-overtone mode Cepheids in the LMC at optical and near-infrared wavelengths by applying the robust statistical tests. We also determine the significance of these observed non-linearities in distance scale applications. The results are summarized as follows-

(i) For fundamental-mode Cepheids, we find that optical band P-L relation and Wesenheit function are non-linear at 10 days. At near-infrared wavelengths, the P-L relations are non-linear around 18 days. It is suggested that the break around 18 days is related to a distinct separation in mean Fourier amplitude parameters around 20 days for longer wavelengths as compared to optical bands. We also observe small but significant evidence of non-linearity in most of the P-W relations. The P-C relations exhibit non-linearity only at the optical wavelengths.

(ii) For first-overtone mode Cepheids, we find a significant non-linearity at 2.5 days for all relations in the optical bands. These results are in good agreement with breaks at maximum and minimum light P-C relations observed in Bhardwaj et al. (2014). Most of the P-L and P-W relations based on a combination of optical and near-infrared magnitudes are linear, while most P-C relations are non-linear.

(iii) The W_{H,K_s} relation for both fundamental and first-overtone mode Cepheid is perfectly linear according to most test statistics. Since the longer wavelengths are less sensitive to extinction and metallicity, this linearity may be useful for future distance scale applications.

(iv) The $W^H_{V,I}$ relation used by the SH0ES project is found to be non-linear according to all test statistics. The Davis test suggest a break around $\log(P) = 1.25$. We re-analyse the SH0ES data and obtain a global slope of -3.212 ± 0.013 based on three calibrators. We note that this slope is consistent with the value derived from LMC variables when considering only short periods or the entire period range, while it is significantly different from the value derived from long-period LMC variables.

(v) We do not find any significant difference in the slope derived from the global fit using linear or non-linear P-L relations, due to the large observational scatter in the distant Cepheid data. Our LMC sample does provide a better constraint on the slope and on the metallicity coefficient of the global-fit solution.

We note that a physical explanation of the observed breaks in the P-L relations is still an open question. Bhardwaj et al. (2014, and references therein) have provided possible theoretical interpretation of observed breaks in period-color and amplitude-color relations based on the interaction between hydrogen ionization front (HIF) and stellar photosphere (SP) at different periods and phases. Moreover, the observed breaks may also be related to the changes in the light curve structure as seen in the Fourier parameters at certain periods. For e.g., the Fourier amplitude parameters for first-overtone mode Cepheids show a sharp dip at 2.5 days at optical bands (Bhardwaj et al. 2014). Similarly, the amplitude parameters show a distinct separation for wavelengths longer than J as compared to optical bands around 20 days (Bhardwaj et al. 2015b). However, a correlation between observed breaks and the changes in the Fourier parameters at various periods needs a further investigation. It will also be important to compare the theoretical light curves generated from stellar pulsation models with observed light curve, quantitatively, to understand the physics behind these non-linearities.

These results will also have an importance from a stellar pulsation and evolution point of view as various non-linearities can be used to place constraints on the mass-luminosity (M-L) relations and instability strip topologies obeyed by Cepheids. Currently, theory suggests that the M-L relation is theoretically predicted to constraint the zero-point of the Period-Luminosity-Color relation for Classical Cepheids and in turn the P-L relation zero point (Bono et al. 1999; Bono, Castellani & Marconi 2000). However, the LMC P-L relation has strong evidence of a break at 10 days with statistically significantly different slopes on either side of 10 days. This is possible because for a fixed M-L relation obeyed by LMC Cepheids, the envelope structure changes with mass and hence with period (Kanbur 1995; Kanbur, Ngeow & Feiden 2007). More specifically, the relative location of the interaction between the SP and HIF changes with period. This changing interaction leads to a physical mechanism that can cause changes in the slope of the P-L and/or P-C relations for a given M-L relation and fixed topology of the instability strip (Kanbur, Ngeow & Buchler 2004; Kanbur & Ngeow 2006; Kanbur, Ngeow & Feiden 2007). The change in the topology of the instability strip with the metal abundance can also cause the difference in slopes of the LMC and SMC Cepheid P-L relations. It is also expected that the metallicity differences lead to different M-L relations obeyed by Cepheids in the Magellanic Clouds, which mainly affects the zero-point. However, each M-L pair has an envelope structure that changes with period and hence a change in the SP/HIF interaction leading to possible changes in the slope of P-L relations. In this sense we feel that the M-L relations and the instability strip boundaries (or topology) are not completely independent of each other.

In a subsequent publication we plan to study P-L relations as a function of pulsation phase to further investigate the effect of non-linearity and possible metallicity dependence on the distance scale. However, we also note that multiphase PL/PC relations for a given galaxy, say the LMC, show considerable changes in linearity, dispersion, slope and zero point (Kanbur & Ngeow 2004). We also intend to investigate the physical mechanism for all these observed breaks in the P-L relations by a rigorous comparison with theoretical models. We believe that the theoretical stellar pulsation modeling of observed non-linearities, in principle, can provide important constraints on theories of stellar evolution and pulsation. In particular, these should be allied with comparison of the Fourier parameters of observed and theoretical Cepheid multiwavelength light curves (Bhardwaj et al. 2015b).

ACKNOWLEDGMENTS

The authors acknowledge the Indo-U.S. Science and Technology Forum for the grant provided to University of Delhi for the Joint Center for Analysis of Variable Star Data. We are very grateful to Adam Riess for his helpful guidance regarding the matrix formalism used to analyze SH0ES data. AB is thankful to the Council of Scientific and Industrial Research, New Delhi, for a Senior Research Fellowship and acknowledges the support from Texas A&M University, where some of this research was carried out. LMM acknowledges support by the United States National Science Foundation through AST grant number 1211603 and by Texas A&M University through a faculty start-up fund and the Mitchell-Heep-Munnerlyn Endowed Career Enhancement Professorship in Physics or Astronomy. HPS thanks University of Delhi for a R&D grant. CCN thanks the funding from Ministry of Science and Technology (Taiwan) under the contract NSC101-2112-M-008-017-MY3 and NSC104-2112-M-008-012-MY3. EEOI thanks Rafael S. de Souza and the Cosmostatistics Initiative (COIN) for insightful suggestions. EEOI is partially supported by the Brazilian agency CAPES (grant number 9229-13-2). This research was supported by the Munich Institute for Astro- and Particle Physics (MI-

APP) of the DFG cluster of excellence "Origin and Structure of the Universe".

REFERENCES

Bhardwaj A., Kanbur S. M., Macri L. M., Singh H. P., Ngeow C.-C., Wagner-Kaiser R., Sarajedini A., 2015a, Accepted in AJ, ArXiv e-prints, 1510.03682
Bhardwaj A., Kanbur S. M., Singh H. P., Macri L. M., Ngeow C.-C., 2015b, MNRAS, 447, 3342
Bhardwaj A., Kanbur S. M., Singh H. P., Ngeow C.-C., 2014, MNRAS, 445, 2655
Bird J. C., Stanek K. Z., Prieto J. L., 2009, ApJ, 695, 874
Bono G., Caputo F., Castellani V., Marconi M., 1999, ApJ, 512, 711
Bono G., Castellani V., Marconi M., 2000, ApJ, 529, 293
Cardelli J. A., Clayton G. C., Mathis J. S., 1989, APJ, 345, 245
Davies R. B., 1987, Biometrika, 74, 33
de Souza R. S. et al., 2015, Astronomy and Computing, 12, 21
Elliott J., de Souza R. S., Krone-Martins A., Cameron E., Ishida E. E. O., Hilbe J., 2015, Astronomy and Computing, 10, 61
García-Varela A., Sabogal B. E., Ramírez-Tannus M. C., 2013, MNRAS, 431, 2278
Hardin J. W., Hilbe J. M., 2012, Generalized Linear Models and Extensions, 3rd Edition, 3rd edn. StataCorp LP
Haschke R., Grebel E. K., Duffau S., 2011, AJ, 141, 158
Humphreys E. M. L., Reid M. J., Moran J. M., Greenhill L. J., Argon A. L., 2013, ApJ, 775, 13
Inno L. et al., 2013, ApJ, 764, 84
Kanbur S., Ngeow C., 2005a, in ESA Special Publication, Vol. 576, The Three-Dimensional Universe with Gaia, Turon C., O'Flaherty K. S., Perryman M. A. C., eds., p. 691
Kanbur S. M., 1995, A&A, 297, L91
Kanbur S. M., Marconi M., Ngeow C., Musella I., Turner M., James A., Magin S., Halsey J., 2010, MNRAS, 408, 695
Kanbur S. M., Ngeow C., Nanthakumar A., Stevens R., 2007, PASP, 119, 512
Kanbur S. M., Ngeow C.-C., 2004, MNRAS, 350, 962
Kanbur S. M., Ngeow C. C., 2005b, in Bulletin of the American Astronomical Society, Vol. 37, American Astronomical Society Meeting Abstracts, p. 132.05
Kanbur S. M., Ngeow C.-C., 2006, MNRAS, 369, 705
Kanbur S. M., Ngeow C.-C., Buchler J. R., 2004, MNRAS, 354, 212
Kanbur S. M., Ngeow C.-C., Feiden G., 2007, MNRAS, 380, 819
Koen C., Kanbur S., Ngeow C., 2007, MNRAS, 380, 1440
Leavitt H. S., Pickering E. C., 1912, Harvard College Observatory Circular, 173, 1
Macri L. M., Ngeow C.-C., Kanbur S. M., Mahzooni S., Smitka M. T., 2015, AJ, 149, 117
Madore B. F., 1982, ApJ, 253, 575
Monson A. J., Freedman W. L., Madore B. F., Persson S. E., Scowcroft V., Seibert M., Rigby J. R., 2012, ApJ, 759, 146
Muggeo V. M., 2008, R News, 8, 20
Muggeo V. M. R., 2003, Statistics in Medicine, 22, 3055
Ngeow C., Kanbur S. M., 2006, ApJ, 650, 180
Ngeow C., Kanbur S. M., Nanthakumar A., 2008, A&A, 477, 621
Ngeow C.-C., Kanbur S. M., Bhardwaj A., Singh H. P., 2015, ApJ, 808, 67
Ngeow C.-C., Kanbur S. M., Neilson H. R., Nanthakumar A., Buonaccorsi J., 2009, ApJ, 693, 691
Ngeow C.-C., Kanbur S. M., Nikolaev S., Buonaccorsi J., Cook K. H., Welch D. L., 2005, MNRAS, 363, 831
Persson S. E., Madore B. F., Krzemiński W., Freedman W. L., Roth M., Murphy D. C., 2004, AJ, 128, 2239
Pietrzyński G. et al., 2013, Nature, 495, 76
Raichoor A., Andreon S., 2012, A&A, 543, A19
Riess A. G. et al., 2011, ApJ, 730, 119
Riess A. G. et al., 2009, ApJ, 699, 539
Ripepi V. et al., 2012, MNRAS, 424, 1807
Sandage A., Tammann G. A., Reindl B., 2004, A&A, 424, 43
Sandage A., Tammann G. A., Reindl B., 2009, A&A, 493, 471
Simon N. R., Kanbur S. M., Mihalas D., 1993, ApJ, 414, 310
Soszynski I. et al., 2008, ACTAA, 58, 163
Tammann G. A., Sandage A., Reindl B., 2003, A&A, 404, 423
Ulaczyk K. et al., 2013, Acta Astronomica, 63, 159

APPENDIX A: TESTIMATOR TABLES

We provide the results of testimator analysis for fundamental and first-overtone mode Cepheids in the Tables A1, A2 and A3. The format of the tables and the meaning of each column header is similar to Table 2. The number of independent and non-overlapping subsets are represented by n. Each subset consist of N number of stars over a period range listed under the column $\log(P)$. The slope of P-L relation in each subset is represented by $\hat{\beta}$. Also, β_0 and β_w denote the initial testimator slope and the updated testimator slope, respectively, after each hypothesis testing. The observed and critical value of t-test statistics are denoted by $|t_{obs}|$ (estimated using equation 6) and t_c (obtained using the theoretical t-distribution for a confidence level of more than 95%), respectively. Finally, k is the ratio of $|t_{obs}|$ and t_c and represents the probability of initial guess of the testimator being true. The value of $k < 1/k > 1$ leads to the decision of acceptance/rejection of the null hypothesis (the slopes are equal in two subsets).

Table A1. Results of the testimator on P-L, P-W and P-C relations for FU mode Cepheids. The OGLE-III data are used in optical band relations.

Band	n	$\log(P)$	N	$\hat{\beta}$	β_0	$\lvert t_{obs}\rvert$	t_c	k	Decision	β_w
V	1	0.39900−0.45900	189	-2.346±0.669	—	—	—	—	—	—
	2	0.45900−0.49200	190	-3.988±1.338	-2.346	1.227	2.765	0.444	Accept H_0	-3.074
	3	0.49200−0.52900	189	-1.890±1.103	-3.074	1.074	2.765	0.388	Accept H_0	-2.615
	4	0.52900−0.57500	192	-3.404±0.819	-2.615	0.964	2.765	0.349	Accept H_0	-2.890
	5	0.57500−0.63600	189	-2.554±0.651	-2.890	0.516	2.765	0.187	Accept H_0	-2.827
	6	0.63600−0.70800	191	-2.809±0.641	-2.827	0.029	2.765	0.011	Accept H_0	-2.827
	7	0.70800−0.85600	188	-2.817±0.332	-2.827	0.030	2.766	0.011	Accept H_0	-2.827
	8	0.85600−1.49200	217	-2.424±0.100	-2.827	4.027	2.761	1.458	Reject H_0	-2.239
I	1	0.39900−0.45900	189	-3.035±0.472	—	—	—	—	—	—
	2	0.45900−0.49200	188	-3.757±0.895	-3.035	0.807	2.766	0.292	Accept H_0	-3.246
	3	0.49200−0.52900	189	-2.316±0.764	-3.246	1.218	2.765	0.440	Accept H_0	-2.837
	4	0.52900−0.57600	193	-3.279±0.561	-2.837	0.789	2.765	0.285	Accept H_0	-2.963
	5	0.57600−0.63600	189	-2.839±0.463	-2.963	0.269	2.765	0.097	Accept H_0	-2.951
	6	0.63600−0.70800	189	-3.155±0.436	-2.951	0.468	2.765	0.169	Accept H_0	-2.985
	7	0.70800−0.86000	193	-3.093±0.215	-2.985	0.502	2.765	0.182	Accept H_0	-3.005
	8	0.86000−1.49200	206	-2.719±0.071	-3.005	4.050	2.763	1.466	Reject H_0	-2.586
J	1	0.39900−0.48900	150	-1.956±0.398	—	—	—	—	—	—
	2	0.48900−0.55500	147	-2.844±0.486	-1.956	1.826	2.610	0.700	Accept H_0	-2.578
	3	0.55500−0.65900	153	-3.199±0.318	-2.578	1.955	2.608	0.750	Accept H_0	-3.043
	4	0.65900−0.83500	150	-2.773±0.208	-3.043	1.299	2.609	0.498	Accept H_0	-2.909
	5	0.83500−1.89700	187	-3.190±0.044	-2.909	6.346	2.602	2.438	Reject H_0	-3.596
H	1	0.39900−0.48900	150	-2.367±0.315	—	—	—	—	—	—
	2	0.48900−0.55500	147	-2.997±0.392	-2.367	1.606	2.610	0.615	Accept H_0	-2.754
	3	0.55500−0.65900	153	-3.239±0.253	-2.754	1.917	2.608	0.735	Accept H_0	-3.111
	4	0.65900−0.83500	150	-2.868±0.172	-3.111	1.411	2.609	0.541	Accept H_0	-2.979
	5	0.83500−1.89700	187	-3.213±0.038	-2.979	6.158	2.602	2.366	Reject H_0	-3.531
K_s	1	0.39900−0.48900	150	-2.584±0.270	—	—	—	—	—	—
	2	0.48900−0.55500	147	-3.006±0.362	-2.584	1.165	2.610	0.446	Accept H_0	-2.772
	3	0.55500−0.65900	153	-3.342±0.219	-2.772	2.599	2.608	0.996	Accept H_0	-3.340
	4	0.65900−0.83500	150	-2.953±0.149	-3.340	2.605	2.609	0.998	Accept H_0	-2.954
	5	0.83500−1.89700	187	-3.261±0.034	-2.954	9.120	2.602	3.504	Reject H_0	-4.032
$W_{V,I}$	1	0.39900−0.45800	190	-3.242±0.299	—	—	—	—	—	—
	2	0.45800−0.49000	185	-2.779±0.537	-3.242	0.862	2.766	0.312	Accept H_0	-3.098
	3	0.49000−0.52600	192	-2.787±0.478	-3.098	0.650	2.765	0.235	Accept H_0	-3.025
	4	0.52600−0.57000	192	-3.834±0.389	-3.025	2.080	2.765	0.752	Accept H_0	-3.633
	5	0.57000−0.62800	191	-3.791±0.290	-3.633	0.544	2.765	0.197	Accept H_0	-3.664
	6	0.62800−0.69500	188	-3.482±0.245	-3.664	0.746	2.766	0.270	Accept H_0	-3.615
	7	0.69500−0.83500	191	-3.565±0.151	-3.615	0.329	2.765	0.119	Accept H_0	-3.609
	8	0.83500−1.49200	237	-3.233±0.042	-3.609	9.062	2.759	3.284	Reject H_0	-2.373
$W_{J,H}$	1	0.39900−0.48900	150	-3.034±0.366	—	—	—	—	—	—
	2	0.48900−0.55500	147	-3.247±0.466	-3.034	0.456	2.610	0.175	Accept H_0	-3.071
	3	0.55500−0.65900	153	-3.306±0.289	-3.071	0.813	2.608	0.312	Accept H_0	-3.144
	4	0.65900−0.83500	150	-3.023±0.172	-3.144	0.706	2.609	0.270	Accept H_0	-3.111
	5	0.83500−1.89700	187	-3.249±0.038	-3.111	3.579	2.602	1.375	Reject H_0	-3.301
W_{J,K_s}	1	0.39900−0.48900	150	-3.016±0.260	—	—	—	—	—	—
	2	0.48900−0.55500	147	-3.115±0.345	-3.016	0.285	2.610	0.109	Accept H_0	-3.027
	3	0.55500−0.65900	153	-3.442±0.200	-3.027	2.078	2.608	0.797	Accept H_0	-3.357
	4	0.65900−0.83500	150	-3.078±0.127	-3.357	2.208	2.609	0.846	Accept H_0	-3.121
	5	0.83500−1.89700	187	-3.310±0.030	-3.121	6.292	2.602	2.418	Reject H_0	-3.579
W_{H,K_s}	1	0.39900−0.48900	150	-3.001±0.339	—	—	—	—	—	—
	2	0.48900−0.55500	147	-3.023±0.468	-3.001	0.048	2.610	0.018	Accept H_0	-3.001
	3	0.55500−0.65900	153	-3.540±0.274	-3.001	1.968	2.608	0.755	Accept H_0	-3.408
	4	0.65900−0.83500	150	-3.117±0.160	-3.408	1.814	2.609	0.695	Accept H_0	-3.206
	5	0.83500−1.89700	187	-3.355±0.032	-3.206	4.599	2.602	1.767	Reject H_0	-3.469
$W_{V,J}$	1	0.39900−0.49800	139	-2.387±0.389	—	—	—	—	—	—
	2	0.49800−0.57000	140	-3.627±0.528	-2.387	2.351	2.611	0.900	Accept H_0	-3.504
	3	0.57000−0.68100	141	-3.604±0.322	-3.504	0.313	2.611	0.120	Accept H_0	-3.516
	4	0.68100−0.89300	140	-3.067±0.146	-3.516	3.072	2.611	1.176	Reject H_0	-2.988

Table A1 : Contd...

Band	n	log(P)	N	$\hat{\beta}$	β_0	$\lvert t_{obs}\rvert$	t_c	k	Decision	β_w
$W_{V,H}$	1	0.39900−0.49800	140	-2.385±0.334	—	—	—	—	—	—
	2	0.49800−0.57000	140	-3.456±0.440	-2.385	2.434	2.611	0.932	Accept H_0	-3.383
	3	0.57000−0.68000	140	-3.685±0.283	-3.383	1.066	2.611	0.408	Accept H_0	-3.506
	4	0.68000−0.89000	140	-3.064±0.135	-3.506	3.266	2.611	1.251	Reject H_0	-2.954
W_{V,K_s}	1	0.39900−0.49800	139	-2.972±0.227	—	—	—	—	—	—
	2	0.49800−0.57000	140	-3.323±0.335	-2.972	1.047	2.611	0.401	Accept H_0	-3.113
	3	0.57000−0.68100	140	-3.485±0.204	-3.113	1.827	2.611	0.700	Accept H_0	-3.373
	4	0.68100−0.89500	141	-3.162±0.099	-3.373	2.129	2.611	0.815	Accept H_0	-3.201
	5	0.89500−1.89700	147	-3.333±0.034	-3.201	3.938	2.610	1.509	Reject H_0	-3.400
$W_{I,J}$	1	0.39900−0.49800	140	-2.354±0.508	—	—	—	—	—	—
	2	0.49800−0.57000	139	-3.835±0.660	-2.354	2.242	2.612	0.859	Accept H_0	-3.625
	3	0.57000−0.68000	140	-3.694±0.414	-3.625	0.167	2.611	0.064	Accept H_0	-3.630
	4	0.68000−0.89000	140	-2.992±0.182	-3.630	3.498	2.611	1.340	Reject H_0	-2.775
$W_{I,H}$	1	0.39900−0.49800	140	-2.643±0.313	—	—	—	—	—	—
	2	0.49800−0.57000	140	-3.685±0.418	-2.643	2.494	2.611	0.955	Accept H_0	-3.638
	3	0.57000−0.68000	139	-3.329±0.267	-3.638	1.158	2.612	0.443	Accept H_0	-3.501
	4	0.68000−0.89000	140	-2.996±0.127	-3.501	3.959	2.611	1.516	Reject H_0	-2.736
W_{I,K_s}	1	0.39900−0.49800	139	-2.976±0.241	—	—	—	—	—	—
	2	0.49800−0.57000	140	-3.251±0.362	-2.976	0.759	2.611	0.291	Accept H_0	-3.056
	3	0.57000−0.68100	140	-3.364±0.207	-3.056	1.485	2.611	0.569	Accept H_0	-3.231
	4	0.68100−0.89500	141	-3.147±0.103	-3.231	0.815	2.611	0.312	Accept H_0	-3.205
	5	0.89500−1.89700	148	-3.346±0.034	-3.205	4.112	2.609	1.576	Reject H_0	-3.428
$W^H_{V,I}$	1	0.39900−0.49800	139	-2.808±0.249	—	—	—	—	—	—
	2	0.49800−0.57000	141	-3.377±0.338	-2.808	1.683	2.611	0.644	Accept H_0	-3.175
	3	0.57000−0.68100	140	-3.373±0.209	-3.175	0.944	2.611	0.362	Accept H_0	-3.246
	4	0.68100−0.89300	140	-3.094±0.108	-3.246	1.411	2.611	0.540	Accept H_0	-3.164
	5	0.89300−1.89700	148	-3.313±0.034	-3.164	4.347	2.609	1.666	Reject H_0	-3.412
$V-I$	1	0.39900−0.45900	190	0.316±0.239	—	—	—	—	—	—
	2	0.45900−0.49100	182	-0.210±0.518	0.316	1.013	2.767	0.366	Accept H_0	0.123
	3	0.49100−0.52800	197	0.244±0.403	0.123	0.301	2.764	0.109	Accept H_0	0.136
	4	0.52800−0.57400	190	0.232±0.320	0.136	0.298	2.765	0.108	Accept H_0	0.147
	5	0.57400−0.63300	187	0.314±0.269	0.147	0.623	2.766	0.225	Accept H_0	0.184
	6	0.63300−0.70100	191	0.445±0.242	0.184	1.075	2.765	0.389	Accept H_0	0.286
	7	0.70100−0.84600	193	0.361±0.111	0.286	0.677	2.765	0.245	Accept H_0	0.304
	8	0.84600−1.49200	226	0.350±0.035	0.304	1.325	2.760	0.480	Accept H_0	0.326
$J-H$	1	0.39900−0.49200	130	0.249±0.148	—	—	—	—	—	—
	2	0.49200−0.56100	130	0.024±0.202	0.249	1.121	2.614	0.429	Accept H_0	0.153
	3	0.56100−0.66600	130	-0.087±0.119	0.153	2.013	2.614	0.770	Accept H_0	-0.032
	4	0.66600−0.83800	129	0.019±0.066	-0.032	0.776	2.614	0.297	Accept H_0	-0.017
	5	0.83800−1.89700	178	0.013±0.014	-0.017	2.142	2.604	0.823	Accept H_0	0.008
$J-K_s$	1	0.39900−0.49400	130	0.368±0.164	—	—	—	—	—	—
	2	0.49400−0.56200	130	-0.213±0.216	0.368	2.689	2.614	1.029	Reject H_0	-0.230
$H-K_s$	1	0.39900−0.49200	130	0.221±0.108	—	—	—	—	—	—
	2	0.49200−0.56100	130	-0.034±0.138	0.221	1.847	2.614	0.707	Accept H_0	0.041
	3	0.56100−0.66500	128	0.047±0.101	0.041	0.066	2.615	0.025	Accept H_0	0.041
	4	0.66500−0.83800	131	0.100±0.048	0.041	1.215	2.614	0.465	Accept H_0	0.068
	5	0.83800−1.89700	177	0.056±0.008	0.068	1.461	2.604	0.561	Accept H_0	0.061
$V-J$	1	0.39900−0.49100	127	0.780±0.398	—	—	—	—	—	—
	2	0.49100−0.55800	132	0.868±0.552	0.780	0.159	2.614	0.061	Accept H_0	0.786
	3	0.55800−0.66500	131	0.782±0.371	0.786	0.011	2.614	0.004	Accept H_0	0.786
	4	0.66500−0.83800	129	0.432±0.231	0.786	1.529	2.614	0.585	Accept H_0	0.579
	5	0.83800−1.89700	178	0.391±0.048	0.579	3.892	2.604	1.495	Reject H_0	0.298
$V-H$	1	0.39900−0.49100	126	1.034±0.445	—	—	—	—	—	—
	2	0.49100−0.55900	134	1.158±0.612	1.034	0.202	2.613	0.077	Accept H_0	1.044
	3	0.55900−0.66500	128	0.983±0.412	1.044	0.148	2.615	0.057	Accept H_0	1.041
	4	0.66500−0.84100	132	0.377±0.249	1.041	2.665	2.614	1.020	Reject H_0	0.364
$V-K_s$	1	0.39900−0.49200	130	1.030±0.409	—	—	—	—	—	—
	2	0.49200−0.55900	129	0.729±0.672	1.030	0.448	2.614	0.171	Accept H_0	0.978
	3	0.55900−0.66600	131	1.117±0.403	0.978	0.345	2.614	0.132	Accept H_0	0.997
	4	0.66600−0.84700	130	0.371±0.241	0.997	2.595	2.614	0.993	Accept H_0	0.375
	5	0.84700−1.89700	173	0.446±0.062	0.375	1.144	2.605	0.439	Accept H_0	0.406

Table A1 : Contd...

Band	n	$\log(P)$	N	$\hat{\beta}$	β_0	$\lvert t_{obs}\rvert$	t_c	k	Decision	β_w
$I-J$	1	0.39900−0.49800	139	0.075±0.232	—	—	—	—	—	—
	2	0.49800−0.57000	138	0.374±0.295	0.075	1.016	2.612	0.389	Accept H_0	0.191
	3	0.57000−0.68200	142	0.261±0.199	0.191	0.350	2.611	0.134	Accept H_0	0.201
	4	0.68200−0.91300	141	0.076±0.096	0.201	1.301	2.611	0.498	Accept H_0	0.138
	5	0.91300−1.89700	141	0.152±0.032	0.138	0.429	2.611	0.164	Accept H_0	0.141
$I-H$	1	0.39900−0.49800	139	0.353±0.277	—	—	—	—	—	—
	2	0.49800−0.57000	138	0.609±0.355	0.353	0.720	2.612	0.276	Accept H_0	0.423
	3	0.57000−0.68300	143	0.074±0.223	0.423	1.563	2.611	0.599	Accept H_0	0.214
	4	0.68300−0.91400	140	0.015±0.115	0.214	1.732	2.611	0.663	Accept H_0	0.082
	5	0.91400−1.89700	140	0.156±0.040	0.082	1.850	2.611	0.708	Accept H_0	0.134
$I-K_s$	1	0.39900−0.49100	126	0.642±0.294	—	—	—	—	—	—
	2	0.49100−0.55900	133	0.551±0.360	0.642	0.253	2.613	0.097	Accept H_0	0.633
	3	0.55900−0.66500	129	0.524±0.255	0.633	0.429	2.614	0.164	Accept H_0	0.615
	4	0.66500−0.84000	132	0.139±0.157	0.615	3.026	2.614	1.158	Reject H_0	0.064

Table A2. Results of the testimator on P-L, P-W and P-C relations for FU mode Cepheids using the OGLE-III-SS data.

Band	n	$\log(P)$	N	$\hat{\beta}$	β_0	$\lvert t_{obs}\rvert$	t_c	k	Decision	β_w
V	1	0.39900−0.45900	189	-2.346±0.669	—	—	—	—	—	—
	2	0.45900−0.49200	190	-3.988±1.338	-2.346	1.227	2.765	0.444	Accept H_0	-3.074
	3	0.49200−0.52900	189	-1.890±1.103	-3.074	1.074	2.765	0.388	Accept H_0	-2.615
	4	0.52900−0.57400	189	-2.969±0.878	-2.615	0.403	2.765	0.146	Accept H_0	-2.666
	5	0.57400−0.63500	193	-2.554±0.666	-2.666	0.168	2.765	0.061	Accept H_0	-2.659
	6	0.63500−0.70500	188	-2.606±0.656	-2.659	0.081	2.766	0.029	Accept H_0	-2.658
	7	0.70500−0.85300	192	-2.750±0.328	-2.658	0.281	2.765	0.102	Accept H_0	-2.667
	8	0.85300−1.71900	238	-2.680±0.074	-2.667	0.168	2.759	0.061	Accept H_0	-2.668
I	1	0.39900−0.45900	189	-3.035±0.472	—	—	—	—	—	—
	2	0.45900−0.49200	189	-3.903±0.911	-3.035	0.953	2.765	0.345	Accept H_0	-3.334
	3	0.49200−0.52900	189	-2.316±0.764	-3.334	1.333	2.765	0.482	Accept H_0	-2.843
	4	0.52900−0.57600	193	-3.279±0.561	-2.843	0.776	2.765	0.281	Accept H_0	-2.966
	5	0.57600−0.63600	189	-2.839±0.463	-2.966	0.275	2.765	0.099	Accept H_0	-2.953
	6	0.63600−0.70800	190	-3.301±0.441	-2.953	0.789	2.765	0.285	Accept H_0	-3.052
	7	0.70800−0.85900	190	-3.115±0.226	-3.052	0.277	2.765	0.100	Accept H_0	-3.059
	8	0.85900−1.71900	230	-2.949±0.052	-3.059	2.124	2.760	0.769	Accept H_0	-2.974
$W_{V,I}$	1	0.39900−0.45800	190	-3.242±0.299	—	—	—	—	—	—
	2	0.45800−0.49000	185	-2.779±0.537	-3.242	0.862	2.766	0.312	Accept H_0	-3.098
	3	0.49000−0.52600	193	-2.767±0.489	-3.098	0.675	2.765	0.244	Accept H_0	-3.017
	4	0.52600−0.57000	192	-3.834±0.389	-3.017	2.099	2.765	0.759	Accept H_0	-3.637
	5	0.57000−0.62700	188	-3.812±0.299	-3.637	0.584	2.766	0.211	Accept H_0	-3.674
	6	0.62700−0.69500	191	-3.462±0.238	-3.674	0.893	2.765	0.323	Accept H_0	-3.605
	7	0.69500−0.83500	191	-3.565±0.151	-3.605	0.265	2.765	0.096	Accept H_0	-3.602
	8	0.83500−1.72400	259	-3.326±0.029	-3.602	9.574	2.757	3.473	Reject H_0	-2.645
$V-I$	1	0.39900−0.45900	190	0.316±0.239	—	—	—	—	—	—
	2	0.45900−0.49100	182	-0.210±0.518	0.316	1.013	2.767	0.366	Accept H_0	0.123
	3	0.49100−0.52800	197	0.244±0.403	0.123	0.301	2.764	0.109	Accept H_0	0.136
	4	0.52800−0.57400	190	0.232±0.320	0.136	0.298	2.765	0.108	Accept H_0	0.147
	5	0.57400−0.63300	187	0.314±0.269	0.147	0.623	2.766	0.225	Accept H_0	0.184
	6	0.63300−0.70100	191	0.445±0.242	0.184	1.075	2.765	0.389	Accept H_0	0.286
	7	0.70100−0.84600	193	0.361±0.111	0.286	0.677	2.765	0.245	Accept H_0	0.304
	8	0.84600−1.72400	249	0.252±0.025	0.304	2.046	2.758	0.742	Accept H_0	0.266

Table A3. Results of the testimator on P-L, P-W and P-C relations for FO mode Cepheids. The OGLE-III data are used in optical band relations.

Band	n	$\log(P)$	N	$\hat{\beta}$	β_0	$\lvert t_{obs}\rvert$	t_c	k	Decision	β_w
V	1	-0.15100−0.18100	210	-3.194±0.118	—	—	—	—	—	—
	2	0.18100−0.28500	208	-2.931±0.447	-3.194	0.588	2.600	0.226	Accept H_0	-3.134
	3	0.28500−0.33700	211	-3.897±0.895	-3.134	0.852	2.599	0.328	Accept H_0	-3.384
	4	0.33700−0.43400	211	-4.285±0.404	-3.384	2.232	2.599	0.859	Accept H_0	-4.158
	5	0.43400−0.77200	232	-2.721±0.136	-4.158	10.606	2.597	4.084	Reject H_0	1.711
I	1	-0.15100−0.18100	209	-3.238±0.087	—	—	—	—	—	—
	2	0.18100−0.28600	210	-3.171±0.310	-3.238	0.216	2.599	0.083	Accept H_0	-3.233
	3	0.28600−0.33700	208	-3.694±0.617	-3.233	0.747	2.600	0.288	Accept H_0	-3.365
	4	0.33700−0.43400	213	-4.013±0.298	-3.365	2.172	2.599	0.836	Accept H_0	-3.906
	5	0.43400−0.77200	231	-2.932±0.097	-3.906	10.012	2.597	3.855	Reject H_0	-0.152
J	1	-0.14100−0.25700	110	-3.435±0.128	—	—	—	—	—	—
	2	0.25700−0.32300	110	-2.335±0.938	-3.435	1.173	2.539	0.462	Accept H_0	-2.927
	3	0.32300−0.38600	110	-4.221±0.717	-2.927	1.806	2.539	0.711	Accept H_0	-3.847
	4	0.38600−0.77200	144	-3.040±0.093	-3.847	8.689	2.529	3.435	Reject H_0	-1.073
H	1	-0.14100−0.25700	110	-3.405±0.105	—	—	—	—	—	—
	2	0.25700−0.32300	110	-2.716±0.658	-3.405	1.046	2.539	0.412	Accept H_0	-3.121
	3	0.32300−0.38600	110	-4.169±0.539	-3.121	1.944	2.539	0.766	Accept H_0	-3.924
	4	0.38600−0.77200	144	-3.068±0.067	-3.924	12.712	2.529	5.026	Reject H_0	0.378
K_s	1	-0.14100−0.25700	110	-3.209±0.094	—	—	—	—	—	—
	2	0.25700−0.32300	110	-3.054±0.560	-3.209	0.277	2.539	0.109	Accept H_0	-3.192
	3	0.32300−0.38600	110	-3.696±0.454	-3.192	1.110	2.539	0.437	Accept H_0	-3.413
	4	0.38600−0.77200	144	-3.138±0.057	-3.413	4.807	2.529	1.900	Reject H_0	-2.890
$W_{V,I}$	1	-0.15100−0.19400	210	-3.429±0.050	—	—	—	—	—	—
	2	0.19400−0.28800	206	-3.754±0.181	-3.429	1.793	2.600	0.690	Accept H_0	-3.653
	3	0.28800−0.34000	209	-3.950±0.321	-3.653	0.925	2.600	0.356	Accept H_0	-3.759
	4	0.34000−0.44100	215	-3.503±0.134	-3.759	1.916	2.599	0.737	Accept H_0	-3.570
	5	0.44100−0.77200	223	-3.388±0.059	-3.570	3.101	2.598	1.194	Reject H_0	-3.352
$W_{J,H}$	1	-0.14100−0.25700	110	-3.355±0.146	—	—	—	—	—	—
	2	0.25700−0.32300	110	-3.334±0.657	-3.355	0.032	2.539	0.013	Accept H_0	-3.355
	3	0.32300−0.38600	110	-4.084±0.666	-3.355	1.095	2.539	0.431	Accept H_0	-3.669
	4	0.38600−0.77200	144	-3.113±0.086	-3.669	6.438	2.529	2.545	Reject H_0	-2.253
W_{J,K_s}	1	-0.14100−0.25700	110	-3.054±0.097	—	—	—	—	—	—
	2	0.25700−0.32300	110	-3.552±0.480	-3.054	1.039	2.539	0.409	Accept H_0	-3.257
	3	0.32300−0.38600	110	-3.335±0.474	-3.257	0.163	2.539	0.064	Accept H_0	-3.262
	4	0.38600−0.77200	144	-3.205±0.056	-3.262	1.019	2.529	0.403	Accept H_0	-3.239
W_{H,K_s}	1	-0.14100−0.25700	110	-2.834±0.138	—	—	—	—	—	—
	2	0.25700−0.32300	110	-3.700±0.683	-2.834	1.268	2.539	0.499	Accept H_0	-3.267
	3	0.32300−0.38600	110	-2.785±0.637	-3.267	0.756	2.539	0.298	Accept H_0	-3.123
	4	0.38600−0.77200	144	-3.272±0.082	-3.123	1.817	2.529	0.718	Accept H_0	-3.230
$W_{V,J}$	1	-0.14100−0.24900	100	-3.483±0.133	—	—	—	—	—	—
	2	0.24900−0.32700	99	-3.947±0.711	-3.483	0.652	2.544	0.256	Accept H_0	-3.602
	3	0.32700−0.39500	100	-3.548±0.665	-3.602	0.082	2.544	0.032	Accept H_0	-3.600
	4	0.39500−0.77200	125	-3.106±0.111	-3.600	4.461	2.534	1.760	Reject H_0	-2.730
$W_{V,H}$	1	-0.14100−0.24900	100	-3.441±0.116	—	—	—	—	—	—
	2	0.24900−0.32800	100	-3.365±0.555	-3.441	0.137	2.544	0.054	Accept H_0	-3.437
	3	0.32800−0.39800	100	-3.474±0.492	-3.437	0.075	2.544	0.029	Accept H_0	-3.438
	4	0.39800−0.77200	123	-3.058±0.090	-3.438	4.227	2.535	1.668	Reject H_0	-2.805
W_{V,K_s}	1	-0.14100−0.25000	100	-3.191±0.089	—	—	—	—	—	—
	2	0.25000−0.32900	100	-3.230±0.410	-3.191	0.096	2.544	0.038	Accept H_0	-3.193
	3	0.32900−0.39900	100	-3.017±0.402	-3.193	0.438	2.544	0.172	Accept H_0	-3.162
	4	0.39900−0.77200	122	-3.152±0.060	-3.162	0.178	2.535	0.070	Accept H_0	-3.162
$W_{I,J}$	1	-0.14100−0.24900	100	-3.454±0.176	—	—	—	—	—	—
	2	0.24900−0.32800	100	-3.724±0.858	-3.454	0.315	2.544	0.124	Accept H_0	-3.487
	3	0.32800−0.39800	100	-2.896±0.847	-3.487	0.697	2.544	0.274	Accept H_0	-3.325
	4	0.39800−0.77200	123	-3.010±0.141	-3.325	2.238	2.535	0.883	Accept H_0	-3.047
$W_{I,H}$	1	-0.14100−0.25000	100	-3.377±0.107	—	—	—	—	—	—
	2	0.25000−0.32900	100	-2.921±0.500	-3.377	0.911	2.544	0.358	Accept H_0	-3.214
	3	0.32900−0.39800	100	-3.082±0.497	-3.214	0.264	2.544	0.104	Accept H_0	-3.200
	4	0.39800−0.77200	122	-3.090±0.071	-3.200	1.554	2.535	0.613	Accept H_0	-3.133

Table A3 : Contd...

Band	n	log(P)	N	$\hat{\beta}$	β_0	$\lvert t_{obs}\rvert$	t_c	k	Decision	β_w
W_{I,K_s}	1	-0.14100−0.25000	100	-3.153±0.094	—	—	—	—	—	—
	2	0.25000−0.33000	99	-3.150±0.396	-3.153	0.008	2.544	0.003	Accept H_0	-3.153
	3	0.33000−0.40300	101	-2.965±0.393	-3.153	0.480	2.543	0.189	Accept H_0	-3.118
	4	0.40300−0.77200	120	-3.145±0.064	-3.118	0.425	2.536	0.168	Accept H_0	-3.122
$W^H_{V,I}$	1	-0.14100−0.25000	100	-3.429±0.086	—	—	—	—	—	—
	2	0.25000−0.32800	100	-3.141±0.414	-3.429	0.695	2.544	0.273	Accept H_0	-3.350
	3	0.32800−0.39500	99	-3.523±0.422	-3.350	0.409	2.544	0.161	Accept H_0	-3.378
	4	0.39500−0.77200	124	-3.148±0.058	-3.378	3.968	2.535	1.566	Reject H_0	-3.019
$V-I$	1	-0.15100−0.18100	210	0.052±0.042	—	—	—	—	—	—
	2	0.18100−0.28500	209	0.242±0.152	0.052	1.244	2.600	0.478	Accept H_0	0.143
	3	0.28500−0.33800	211	-0.112±0.311	0.143	0.821	2.599	0.316	Accept H_0	0.063
	4	0.33800−0.43300	210	-0.158±0.157	0.063	1.406	2.599	0.541	Accept H_0	-0.057
	5	0.43300−0.77200	234	0.273±0.047	-0.057	7.007	2.597	2.698	Reject H_0	0.832
$J-H$	1	-0.14100−0.25700	100	-0.089±0.061	—	—	—	—	—	—
	2	0.25700−0.33200	99	0.038±0.248	-0.089	0.514	2.544	0.202	Accept H_0	-0.063
	3	0.33200−0.40800	101	-0.103±0.229	-0.063	0.171	2.543	0.067	Accept H_0	-0.066
	4	0.40800−0.77200	111	-0.011±0.049	-0.066	1.112	2.539	0.438	Accept H_0	-0.042
$J-K_s$	1	-0.14100−0.25700	100	-0.257±0.057	—	—	—	—	—	—
	2	0.25700−0.33300	100	0.327±0.263	-0.257	2.218	2.544	0.872	Accept H_0	0.252
	3	0.33300−0.41100	100	-0.208±0.238	0.252	1.938	2.544	0.762	Accept H_0	-0.099
	4	0.41100−0.77200	107	0.100±0.052	-0.099	3.787	2.541	1.491	Reject H_0	0.197
$H-K_s$	1	-0.13400−0.26100	100	-0.143±0.049	—	—	—	—	—	—
	2	0.26100−0.33300	100	0.265±0.213	-0.143	1.913	2.544	0.752	Accept H_0	0.164
	3	0.33300−0.40700	100	-0.071±0.187	0.164	1.254	2.544	0.493	Accept H_0	0.048
	4	0.40700−0.77200	115	0.059±0.037	0.048	0.313	2.538	0.123	Accept H_0	0.049
$V-J$	1	-0.14100−0.25600	99	0.036±0.130	—	—	—	—	—	—
	2	0.25600−0.33300	101	0.187±0.654	0.036	0.231	2.543	0.091	Accept H_0	0.050
	3	0.33300−0.41400	100	0.170±0.570	0.050	0.211	2.544	0.083	Accept H_0	0.060
	4	0.41400−0.77200	108	0.426±0.137	0.060	2.667	2.540	1.050	Reject H_0	0.444
$V-H$	1	-0.14100−0.25600	99	-0.028±0.146	—	—	—	—	—	—
	2	0.25600−0.33300	100	0.204±0.757	-0.028	0.307	2.544	0.121	Accept H_0	-0.000
	3	0.33300−0.41500	101	-0.262±0.581	-0.000	0.450	2.543	0.177	Accept H_0	-0.046
	4	0.41500−0.77200	104	0.356±0.136	-0.046	2.964	2.542	1.166	Reject H_0	0.423
$V-K_s$	1	-0.14100−0.25600	100	-0.277±0.155	—	—	—	—	—	—
	2	0.25600−0.33300	100	0.525±0.778	-0.277	1.031	2.544	0.405	Accept H_0	0.048
	3	0.33300−0.41400	100	-0.290±0.635	0.048	0.533	2.544	0.209	Accept H_0	-0.023
	4	0.41400−0.77200	105	0.412±0.145	-0.023	3.007	2.541	1.183	Reject H_0	0.491
$I-J$	1	-0.14100−0.26100	100	0.022±0.083	—	—	—	—	—	—
	2	0.26100−0.33400	99	-0.511±0.366	0.022	1.457	2.544	0.573	Accept H_0	-0.284
	3	0.33400−0.42000	101	0.201±0.314	-0.284	1.543	2.543	0.607	Accept H_0	0.010
	4	0.42000−0.77200	103	0.191±0.083	0.010	2.178	2.542	0.857	Accept H_0	0.165
$I-H$	1	-0.14100−0.25800	100	-0.079±0.092	—	—	—	—	—	—
	2	0.25800−0.33300	98	-0.531±0.469	-0.079	0.964	2.545	0.379	Accept H_0	-0.250
	3	0.33300−0.41600	102	-0.360±0.354	-0.250	0.310	2.543	0.122	Accept H_0	-0.264
	4	0.41600−0.77200	103	0.131±0.081	-0.264	4.860	2.542	1.912	Reject H_0	0.491
$I-K_s$	1	-0.14100−0.25600	100	-0.308±0.104	—	—	—	—	—	—
	2	0.25600−0.33300	99	-0.035±0.465	-0.308	0.587	2.544	0.231	Accept H_0	-0.245
	3	0.33300−0.41500	101	-0.298±0.383	-0.245	0.139	2.543	0.054	Accept H_0	-0.248
	4	0.41500−0.77200	104	0.203±0.092	-0.248	4.903	2.542	1.929	Reject H_0	0.621